A chemical screen based on an interruption of zebrafish gastrulation identifies the HTR2C inhibitor Pizotifen as a suppressor of EMT-mediated metastasis

Joji Nakayama[1,2,3,4,§], Lora Tan[1], Boon Cher Goh[2], Shu Wang[1, 5], Hideki Makinoshima[3,6] and Zhiyuan Gong[1,§]

[1]Department of Biological Science, National University of Singapore, Singapore
[2]Cancer Science Institute of Singapore, National University of Singapore, Singapore
[3]Tsuruoka Metabolomics Laboratory, National Cancer Center, Tsuruoka, Japan
[4]Shonai Regional Industry Promotion Center, Tsuruoka, Japan.
[5]Institute of Bioengineering and Nanotechnology, Singapore
[6]Division of Translational Research, Exploratory Oncology Research and Clinical Trial Center, National Cancer Center, Kashiwa, Japan.

[§]Corresponding authors:
Joji Nakayama
email: Zmetastasis@gmail.com

Zhiyuan Gong
email: dbsgzy@nus.edu.sg

Keywords: Metastasis, gastrulation, EMT, Phenotyping screening, zebrafish

Total words excluding supplemental figure legends and references section: 5468

Number of figures: 5
Number of tables: 1
Number of supplemental figures: 3
Number of supplemental tables: 6

Abstract

Metastasis is responsible for approximately 90% of cancer-associated mortality but few models exist that allow for rapid and effective screening of anti-metastasis drugs. Current mouse models of metastasis are too expensive and time consuming to use for rapid and high-throughput screening. Therefore, we created a unique screening concept utilizing conserved mechanisms between zebrafish gastrulation and cancer metastasis for identification of potential anti-metastatic drugs. We hypothesized that small chemicals that interrupt zebrafish gastrulation might also suppress metastatic progression of cancer cells and developed a phenotype-based chemical screen to test the hypothesis. The screen used epiboly, the first morphogenetic movement in gastrulation, as a marker and enabled 100 chemicals to be tested in five hours. The screen tested 1280 FDA-approved drugs and identified Pizotifen, an antagonist for serotonin receptor 2C (HTR2C) as an epiboly-interrupting drug. Pharmacologic and genetic inhibition of HTR2C suppressed metastatic progression in a mouse model. Blocking HTR2C with Pizotifen restored epithelial properties to metastatic cells through inhibition of Wnt-signaling. In contrast, HTR2C induced epithelial to mesenchymal transition (EMT) through activation of Wnt-signaling and promoted metastatic dissemination of human cancer cells in a zebrafish xenotransplantation model. Taken together, our concept offers a novel platform for discovery of anti-metastasis drugs.

Introduction

Metastasis, a leading contributor to the morbidity of cancer patients, occurs through multiple steps: invasion, intravasation, extravasation, colonization, and metastatic tumor formation (1-3). The physical translocation of cancer cells is an initial step of metastasis and molecular mechanisms of it involve cell motility, the breakdown of local basement membrane, loss of cell polarity, acquisition of stem cell-like properties, and EMT (4-6). These cell-biological phenomena are also observed during vertebrate gastrulation in that evolutionarily conserved morphogenetic movements of epiboly, internalization, convergence, and extension progress (7). In zebrafish, the first morphogenetic movement, epiboly, is initiated at approximately 4 hours post fertilization (hpf) to move cells from the animal pole to eventually engulf the entire yolk cell by 10 hpf (8, 9). The embryonic cell movements are governed by the molecular mechanisms that are partially shared in metastatic cell dissemination.

At least fifty common genes were shown to be involved in both metastasis and gastrulation progression: Knockdown of these genes in Xenopus or zebrafish induced gastrulation defects; conversely, overexpression of these genes conferred metastatic potential on cancer cells and knockdown of these genes suppressed metastasis (Table S1). This evidence led us to hypothesize that small molecules that interrupt zebrafish gastrulation may suppress metastatic progression of human cancer cells.

Here we report a unique screening concept based on the hypothesis. Pizotifen, an antagonist for HTR2C, was identified from the screen as a “hit” that interrupted zebrafish gastrulation. A mouse model of metastasis confirmed pharmacological and genetic inhibition of HTR2C suppressed metastatic progression. Moreover, HTR2C induced EMT and promoted metastatic dissemination of non-metastatic cancer cells in a zebrafish xenotransplantation model. These results demonstrated that this concept could offer a novel high-throughput platform for discovery of anti-metastasis drugs and can be converted to a chemical genetic screening platform.

Results

Small molecules interrupting epiboly of zebrafish have a potential to suppress metastatic progression of human cancer cells.

Before performing a screening assay, we conducted preliminary experiments to test the hypothesis. First, we examined whether hindering the molecular function of reported genes, whose knockdown induced gastrulation defects in zebrafish, might suppress cell motility and invasion of cancer cells. We chose protein arginine methyltransferase 1 (PRMT1) and cytochrome P450 family 11 (CYP11A1), both of whose knockdown induced gastrulation defects in zebrafish but whose involvement in metastatic progression is unclear (10, 11). Elevated expression of PRMT1 and CYP11A1 were observed in highly metastatic human breast cancer cell lines and knockdown of these genes through RNA interference suppressed the motility and invasion of MDA-MB-231 cells without affecting their viability (Figure S1A-C).

Next, we conducted an inverse examination of whether chemicals which were reported to suppress metastatic dissemination of cancer cells could interrupt epiboly progression of zebrafish embryos. Niclosamide and Vinpocetine are reported to suppress metastatic progression (12, 13) (14, 15). Either Niclosamide or Vinpocetine-treated zebrafish embryos showed complete arrest at very early stages or severe delay in epiboly progression, respectively (Figure S1D).

These results suggest that epiboly could serve as a marker for this screening assay and epiboly-interrupting drugs that are identified through this screening could have the potential to suppress metastatic progression of human cancer cells.

132 FDA-approved drugs induced delayed in epiboly of zebrafish embryos

We screened 1,280 FDA, EMA or other agencies-approved drugs (Prestwick, Inc) in our zebrafish assay. The screening showed that 0.9% (12/1280) of the drugs, including Actimycin A and Tolcapone, induced severe or complete arrest of embryonic cell

movement when embryos were treated with 10μM. 5.2% (66/1280) of the drugs, such as Dicumarol, Racecadotril, Pizotifen and S(-) Eticlopride hydrochloride, induced either delayed epiboly or interrupted epiboly of the embryos. 93.3% (1194/1280) of drugs has no effect on epiboly progression of the embryos. 0.6% (8/1280) of drugs induced a toxic lethality. Epiboly progression was affected more severely when embryos were treated with 50μM; 1.7% (22/1280) of the drugs induced severe or complete arrest of it. 8.6% (110/1280) of the drugs induced either delayed epiboly or interrupt epiboly of the embryos. 4.3% (55/1280) of drugs induced a toxic lethality (Figure 1A and 1B, Table S2). Among the epiboly-interrupting drugs, several drugs have already been reported to inhibit metastasis-related molecular mechanisms: Adrenosterone or Zardaverine, which target HSD11β1 or PDE3 and 4, respectively, are reported to inhibit EMT (16, 17); Racecadotril, which targets enkephalinase, is reported to confer metastatic potential on colon cancer cell (18); and Disulfiram, which targets ALDH, is reported to confer stem-like properties on metastatic cancer cells (19). This evidence suggests that epiboly-interrupting drugs have the potential for suppressing metastasis of human cancer cells.

Identified drugs suppressed cell motility and invasion of human cancer cells.

It has been reported that zebrafish have orthologues to 86% of 1318 human drug targets (20). However, it was not known whether the epiboly-interrupting drugs could suppress metastatic dissemination of human cancer cells. To test this, we subjected the 78 epiboly-interrupting drugs that showed a suppressor effect on epiboly progression at a 10μM concentration to *in vitro* experiments using a human cancer cell line. The experiments examined whether the drugs could suppress cell motility and invasion of MDA-MB-231 cells through a Boyden chamber. Before conducting the experiment, we investigated whether these drugs might effect viability of MDA-MB-231 cells using an MTT assay. Sixteen of the 78 drugs strongly effected cell viability at concentrations less than 1μM and were not used in the cell motility experiments. The remaining 62 drugs were assayed

in Boyden chamber motility experiments. Twenty of the 62 drugs inhibited cell motility and invasion of MDA-MB-231 cells without effecting cell viability. Among the 20 drugs, Hexachlorophene and Nitazoxanide were removed since the primary targets of the drugs, D-lactate dehydrogenase and pyruvate ferredoxin oxidoreductase are not expressed in mammalian cells. With the exception of Ipriflavone, whose target is still unclear, the known primary targets of the remaining 17 drugs are reported to be expressed by mammalian cells (Figure 2A and Table 1).

We confirmed if highly metastatic human cancer cell lines expressed the genes that code for these targets using Western blotting analyses. Among the genes, serotonin receptor 2C (HTR2C), which is a primary target of Pizotifen, was highly expressed in only metastatic cell lines (Figure 2B). Pizotifen suppressed cell motility and invasion of several highly metastatic human cancer cell lines in a dose-dependent manner (Figure 2C). Similarly, Dopamine receptor D2 (DRD2), which is a primary target of S(-) Eticlopride hydrochloride, was highly expressed in only metastatic cell lines, and the drug suppressed cell motility and invasion of these cells in a dose-dependent manner (Figure S2).

These results indicate that a number of the epiboly-interrupting drugs also have suppressor effects on cell motility and invasion of highly metastatic human cancer cells.

Pizotifen suppressed metastatic dissemination of human cancer cells in a zebrafish xenotransplantation model.

While a number of the epiboly-interrupting drugs suppressed cell motility and invasion of human cell lines *in vitro,* it was still unclear whether the drugs could suppress metastatic dissemination of cancer cells in vivo. Therefore, we examined whether the identified drugs could suppress metastatic dissemination of these human cancer cells in a zebrafish xenotransplantation model. Pizotifen was selected to test since HTR2C was overexpressed only in highly metastatic cell lines supporting the hypothesis that it could be a novel target

for blocking metastatic dissemination of cancer cells (Figure 2B). Red fluorescent protein-labelled MDA-MB-231 (231R) cells were injected into the duct of Cuvier of *Tg (kdrl:eGFP)* zebrafish at 2 dpf and then maintained in the presence of either vehicle or Pizotifen. Twenty-four hours post-injection, the numbers of fish showing metastatic dissemination of 231R cells were measured via fluorescence microscopy. In this model, the dissemination patterns were generally divided into three categories: (i) head dissemination, in which disseminated 231R cells exist in the vessel of the head part; (ii) trunk dissemination, in which the cells were observed in the vessel dilating from the trunk to the tail; (iii) end-tail dissemination, in which the cells were observed in the vessel of the end-tail part (16).

Three independent experiments revealed that the frequencies of fish in the drug-treated group showing head, trunk, or end-tail dissemination, significantly decreased to 55.3±7.5%, 28.5±5.0% or 43.5±19.1% when compared with those in the vehicle-treated group; 95.8±5.8%, 47.1±7.7% or 82.6±12.7%. Conversely, the frequency of the fish in the drug-treated group not showing any dissemination, significantly increased to 45.4±0.5% when compared with those in the vehicle-treated group; 2.0±2.9% (Figure 2D and Table S3).

Similar effects were observed in another xenograft experiments using an RFP-labelled human pancreatic cancer cell line, MIA-PaCa-2 (MP2R). In the drug treated group, the frequencies of the fish showing head, trunk or end-tail dissemination, significantly decreased to 15.3±6.7%, 6.2±1.3%, or 41.1±1.5%; conversely, the frequency of the fish not showing any dissemination significantly increased to 46.3±8.9% when compared with those in the vehicle-treated group; 74.5±11.1%, 18.9±14.9%, 77.0±9.0%, or 17.2±0.7% (Figure S3 and Table S4).

To eliminate the possibility that the metastasis suppressing effects of Pizotifen might result from off-target effects of the drug, we conducted validation experiments to determine whether knockdown of HTR2C would show the same effects. Sub-clones of

231R cells that expressed shRNA targeting either LacZ or HTR2C were injected into the fish at 2 dpf and the fish were maintained in the absence of drug. In the fish that were inoculated with shHTR2C 231R cells, the frequencies of the fish showing head, trunk, and end-tail dissemination, significantly decreased to 6.7±4.9%, 6.7±0.7%, or 20.0±16.5%; conversely, the frequency of the fish not showing any dissemination, significantly increased to 80.0±4.4% when compared with those that were inoculated with shLacZ 231R cells; 80.0±27.1%, 20.0±4.5%, 90.0± 7.7%, or 0% (Figure 2E and Table S5).

These results indicate that pharmacological and genetic inhibition of HTR2C suppressed metastatic dissemination of human cancer cells in vivo.

Pizotifen suppressed metastasis progression of a mouse model of metastasis.

We examined the metastasis-suppressor effect of Pizotifen in a mouse model of metastasis (21). Luciferase-expressing 4T1 murine mammary carcinoma cells were inoculated into the mammary fat pads (MFP) of female BALB/c mice. On day two post inoculation, the mice were randomly assigned to two groups and one group received once daily intraperitoneal injections of 10mg/kg Pizotifen while the other group received a vehicle injection. Bioluminescence imaging and tumor measurement revealed that the sizes of the primary tumors in Pizotifen-treated mice were equal to those in the vehicle-treated mice at the time of resection on day 10 post inoculation. Immunofluorescent staining also demonstrated that the percentage of Ki67 positive cells in the resected primary tumors of Pizotifen-treated mice were the same as those of vehicle-treated mice (Figure 3A-C), additionally, both groups showed less than 1% cleaved caspase 3 positive cells (data not shown). Therefore, no anti-tumor effect of Pizotifen was observed on the primary tumor. After 70 days from inoculation, bioluminescence imaging detected light emitted in the lungs, livers and lymph nodes of vehicle-treated mice but not those of Pizotifen-treated mice (Figure 3C). Vehicle-treated mice formed 5 to 50 metastatic

nodules per lung in all 10 mice analyzed; conversely, Pizotifen-treated mice (n=10) formed 0 to 5 nodules per lung in all 10 mice analyzed (Figure 3D). Histological analyses confirmed that metastatic lesions in the lungs were detected in all vehicle-treated mice; conversely, they were detected in only 2 of 10 Pizotifen-treated mice and the rest of the mice showed metastatic colony formations around the bronchiole of the lung. In addition, 4 of 10 vehicle-treated mice exhibited metastasis in the liver and the rest showed metastatic colony formation around the portal tract of the liver. In contrast, none of 10 Pizotifen-treated mice showed liver metastases and only half of the 10 mice showed metastatic colony formation around the portal tract (Figure 3E). These results indicate that Pizotifen can suppress metastasis progression without affecting primary tumor growth.

To eliminate the possibility that the metastasis suppressing effects of Pizotifen might result from off-target effects, we conducted validation experiments to determine whether knockdown of HTR2C would show the same effects. The basic experimental process followed the experimental design described above except that sub-clones of 4T1 cells that expressed shRNA targeting either LacZ or HTR2C were injected into the MFP of female BALB/c mice and the mice were maintained without drug. Histological analyses revealed that all of the mice (n=5) that were inoculated with 4T1 cells expressing shRNA targeting LacZ showed metastases in the lungs. The mean number of metastatic lesions in a lung was 26.4±7.8. In contrast, only one of the mice (n=5) were inoculated with 4T1 cells expressing shRNA targeting HTR2C showed metastases in the lungs and the rest of the mice showed metastatic colony formation around the bronchiole of the lung. The mean number of metastatic lesions in the lung significantly decreased to 10% of those of mice that were inoculated with 4T1 cells expressing shRNA targeting LacZ (Figure 3F-H).

Taken together, pharmacological and genetic inhibition of HTR2C showed an anti-metastatic effect in the 4T1 model system.

HTR2C promoted EMT-mediated metastatic dissemination of human cancer cells

Although pharmacological and genetic inhibition of HTR2C inhibited metastasis progression, a role for HTR2C on metastatic progression has not been reported. Therefore, we examined whether HTR2C could confer metastatic properties on poorly metastatic cells.

Firstly, we established a stable sub-clone of MCF7 human breast cancer cells expressing either vector control or HTR2C. Vector control expressing MCF7 cells maintained highly organized cell-cell adhesion and cell polarity; however, HTR2C-expressing MCF7 cells led to loss of cell-cell contact and cell scattering. The cobblestone-like appearance of these cells was replaced by a spindle-like, fibroblastic morphology. Western blotting and immunofluorescence (IF) analyses revealed that HTR2C-expressing MCF7 cells showed loss of E-cadherin and EpCAM, and elevated expressions of N-cadherin, vimentin and an EMT-inducible transcriptional factor Zeb1. Similar effects were validated through another experiment using an immortal keratinocyte cell line, HaCaT cells, in that HTR2C-expressing HaCaT cells also showed loss of cell-cell contact and cell scattering with loss of epithelial markers and gain of mesenchymal markers (Figure 4A-C). Therefore, both the morphological and molecular changes in the HTR2C-expressing MCF7 and HaCaT cells demonstrated that these cells had undergone an EMT.

Next, we examined whether HTR2C-driven EMT could promote metastatic dissemination of human cancer cells. Boyden chamber assay revealed that HTR2C expressing MCF7 cells showed an increased cell motility and invasion compared with vector control-expressing MCF7 cells in vitro (Figure 4D). Moreover, we conducted in vivo examination of whether HTR2C expression could promote metastatic dissemination of human cancer cells in a zebrafish xenotransplantation model. Red fluorescence protein-labelled MCF7 cells expressing either vector control or HTR2C were injected into the duct of Cuvier of *Tg* (*kdrl:eGFP*) zebrafish at 2 dpf. Twenty-four hours post injection, the frequencies of the fish showing metastatic dissemination of the inoculated cells were

measured using fluorescence microscopy. In the fish that were inoculated with HTR2C expressing MCF7 cells, the frequencies of the fish showing head, trunk, and end-tail dissemination significantly increased to 96.7±4.7%, 68.8±6.4%, or 89.5±3.4%; conversely, the frequency of the fish not showing any dissemination decreased to 0% when compared with those in the fish that were inoculated with vector control expressing MCF7 cells; 33.1±18.5%, 0%, 56.9± 4.4%, or 43% (Figure 4E and Table S6).

These results indicated that HTR2C promoted metastatic dissemination of cancer cells though induction of EMT, and suggest that the screen can easily be converted to a chemical genetic screening platform.

Pizotifen induced mesenchymal to epithelial transition through inhibition of Wnt-signaling.

Finally, we elucidated the mechanism of action of how Pizotifen suppressed metastasis, especially metastatic dissemination of cancer cells. Our results showed that HTR2C induced EMT and that pharmacological and genetic inhibition of HTR2C suppressed metastatic dissemination of MDA-MB-231 cells that had already transitioned to mesenchymal-like traits via EMT. Therefore, we speculated that blocking HTR2C with Pizotifen might inhibit the molecular mechanisms which follow EMT induction. We firstly investigated the expressions of epithelial and mesenchymal markers in Pizotifen-treated MDA-MB-231 cells since the activation of an EMT program needs to be transient and reversible, and transition from a fully mesenchymal phenotype to a epithelial-mesenchymal hybrid state or a fully epithelial phenotype is associated with malignant phenotypes (22). IF and FACS analyses revealed 20% of Pizotifen-treated MDA-MB-231 cells restored E-cadherin expression. Also, western blotting analysis demonstrated that 4T1 primary tumors from Pizotifen-treated mice has elevated E-cadherin expression compared with tumors from vehicle-treated mice (Figure 5A-C). However, mesenchymal markers did not change between vehicle and Pizotifen-treated MDA-MB-231 cells (data

not shown). We further analyzed E-cadherin positive (E-cad$^+$) cells in Pizotifen-treated MDA-MB-231 cells. The E-cad$^+$ cells showed elevated expressions of epithelial markers KRT14 and KRT19; and decreased expression of mesenchymal makers vimentin, MMP1, MMP3, and S100A4. Recent research reports that an EMT program needs to be transient and reversible and that a mesenchymal phenotype in cancer cells is achieved by constitutive ectopic expression of Zeb1. In accordance with the research, the E-cad$^+$ cells and 4T1 primary tumors from Pizotifen-treated mice had decreased Zeb1 expression compared with vehicle-treated cells and tumors from vehicle-treated mice (Figure 5D). In contrast, HTR2C-expressing MCF7 and HuMEC cells expressed Zeb1 but not vehicle control MCF7 and HuMEC cells (Figure 4C). These results indicate that HTR2C-mediated signaling induced EMT through up-regulation of Zeb1 and blocking HTR2C with Pizotifen induced mesenchymal to epithelial transition through downregulation of Zeb1.

We further investigated the mechanism of action of how blocking HTR2C with Pizotifen induced down-regulation of Zeb1. In embryogenesis, serotonin-mediated signaling is required for Wnt-dependent specification of the superficial mesoderm during gastrulation (23). In cancer cells, overexpression of HTR1D is associated with Wnt-signaling which enables induction of EMT (24, 25). This evidence led to a hypothesis that HTR2C-mediated signaling might turn on transcriptional activity of β-catenin and that might induce up-regulation of EMT-TFs. IF analyses revealed β-catenin was accumulated in the nucleus of HTR2C-expressing MCF7 cells but it was located in the cytoplasm of vector control-expressing cells (Figure 5E). Nuclear accumulation of β-catenin in HTR2C-expressing MCF7 cells was confirmed by western blot (Figure 5F). In contrast, Pizotifen-treated MDA-MB-231 cells showed β-catenin located in the cytoplasm of the cells. Vehicle-treated cells showed β-catenin accumulated in the nucleus of the cells. (Figure 5G), and western blotting analysis confirmed that it was located in the cytoplasm of Pizotifen-treated MDA-MB-231 cells (Figure 5H). Furthermore,

318 immunohistochemistry and western blotting analyses showed that β-catenin accumulated
319 in the nucleus, and phospho-GSKβ and Zeb1 expression were decreased in 4T1 primary
320 tumors from Pizotifen-treated mice compared with vehicle-treated mice (Figure 5C).
321 These results indicated that HTR2C would regulate transcriptional activity of β-catenin
322 and Pizotifen could inhibit it.
323 Taken together, we conclude that blocking HTR2C with Pizotifen restored
324 epithelial properties to metastatic cells (MDA-MB-231 and 4T1 cells) through a decrease
325 of transcriptional activity of β-catenin and that suppressed metastatic progression of the
326 cells.
327

328 **Figures and figure legends**

329 **Figure 1**

330

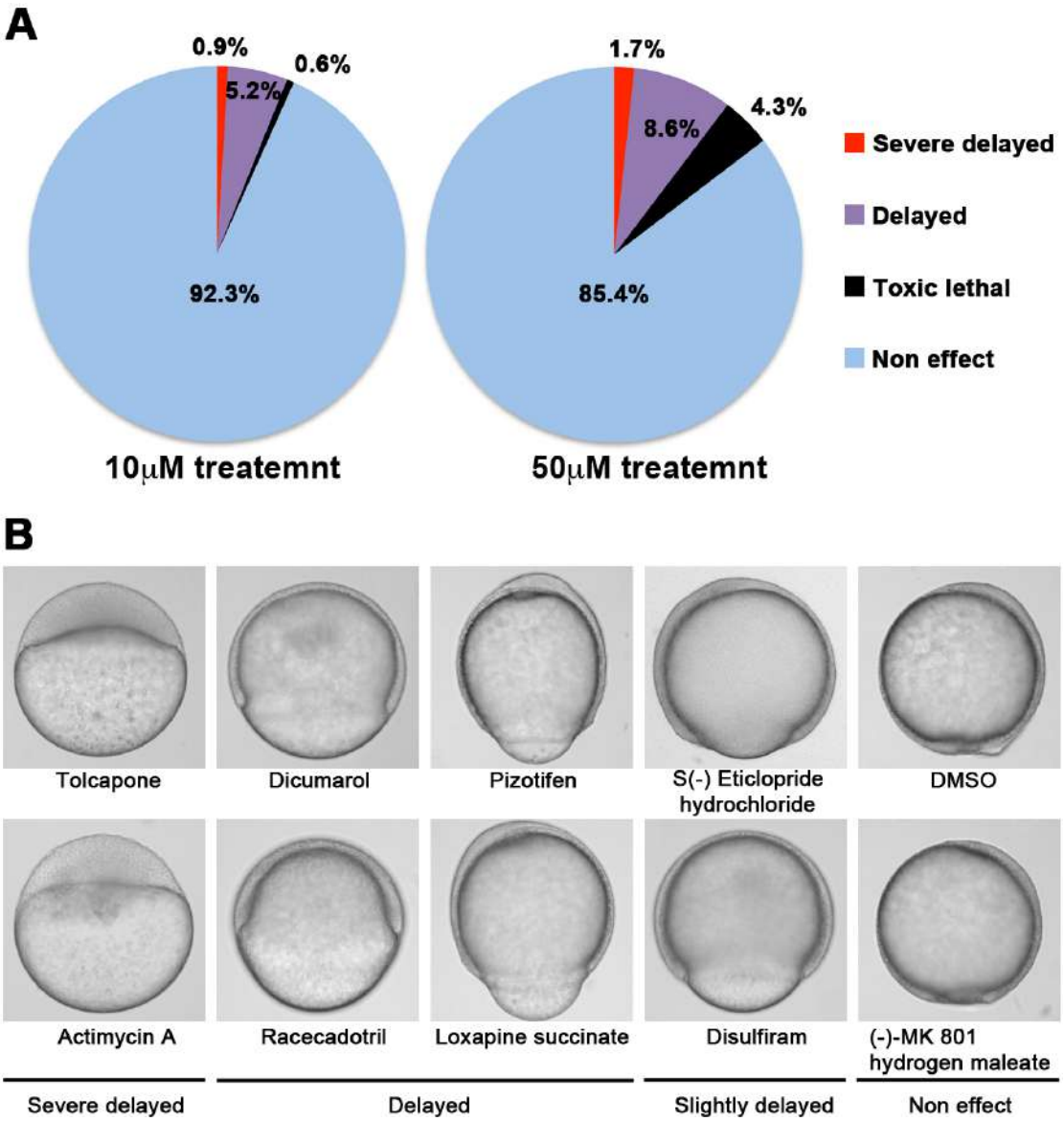

331

332

333 **Figure 1. A chemical screen for identification of epiboly-interrupting drugs.**

334 (A) Cumulative results of the chemical screen in which each drug was used at either

335 10μM (left) or 50μM (right) concentrations. 1,280 FDA, EMA or other agencies-

336 approved drugs were subjected to this screening. Positive "hit" drugs were those that

337 interrupted epiboly progression. (B) Representative samples of the embryos that were

338 treated with indicated drugs.

339 **Figure 2**

340

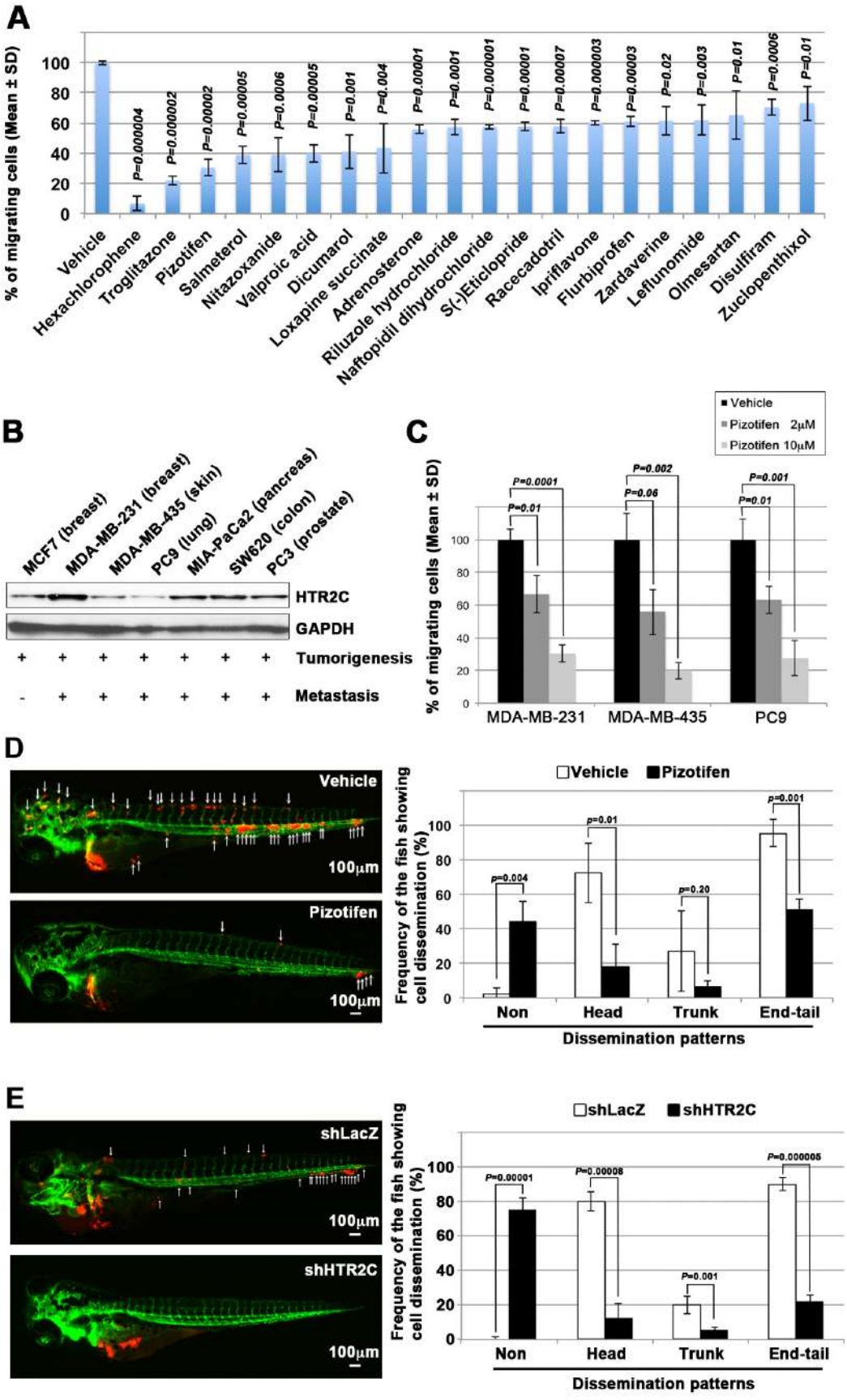

341

342 **Figure 2. Pizotifen, one of epiboly-interrupting drugs suppressed metastatic**

343 **dissemination of human cancer cells lines in vivo and vitro.**

(A) Effect of the epiboly-interrupting drugs on cell motility and invasion of MBA-MB-231 cells. MBA-MB-231 cells were treated with vehicle or each of the epiboly-interrupting drugs and then subjected to Boyden chamber assays. Fetal bovine serum (1%v/v) was used as the chemoattractant in both assays. Each experiment was performed at least twice. (B) Western blot analysis of HTR2C levels (top) in a non-metastatic human cancer cell line, MCF7 (breast) and highly metastatic human cancer cell lines, MDA-MB-231 (breast), MDA-MB-435 (melanoma), PC9 (lung), MIA-PaCa2 (pancreas), PC3 (prostate) and SW620 (colon); GAPDH loading control is shown (bottom). (C) Effect of pizotifen on cell motility and invasion of MBA-MB-231, MDA-MB-435 and PC9 cells. Either vehicle or pizotifen treated the cells were subjected to Boyden chamber assays. Fetal bovine serum (1%v/v) was used as the chemoattractant in both assays. Each experiment was performed at least twice. (D) and (E) Representative images of dissemination of 231R, shLacZ 231R or shHTR2C 231R cells in zebrafish xenotransplantation model. The fish larvae that were inoculated with 231R cells, were treated with either vehicle (top left) or the drug (lower left) (D). The fish larvae that were inoculated with either shLacZ 231R or shHTR2C 231R cells (lower left) (E). White arrows head indicate disseminated 231R cells. The images were shown in 4x magnification. Scale bar, 100μm. The mean frequencies of the fish showing head, trunk, or end-tail dissemination were counted (graph on right). Each value is indicated as the mean ± SEM of two independent experiments. Statistical analysis was determined by Student's t test. See also Figure S2 and S3, Table S3-S5.

Figure 3

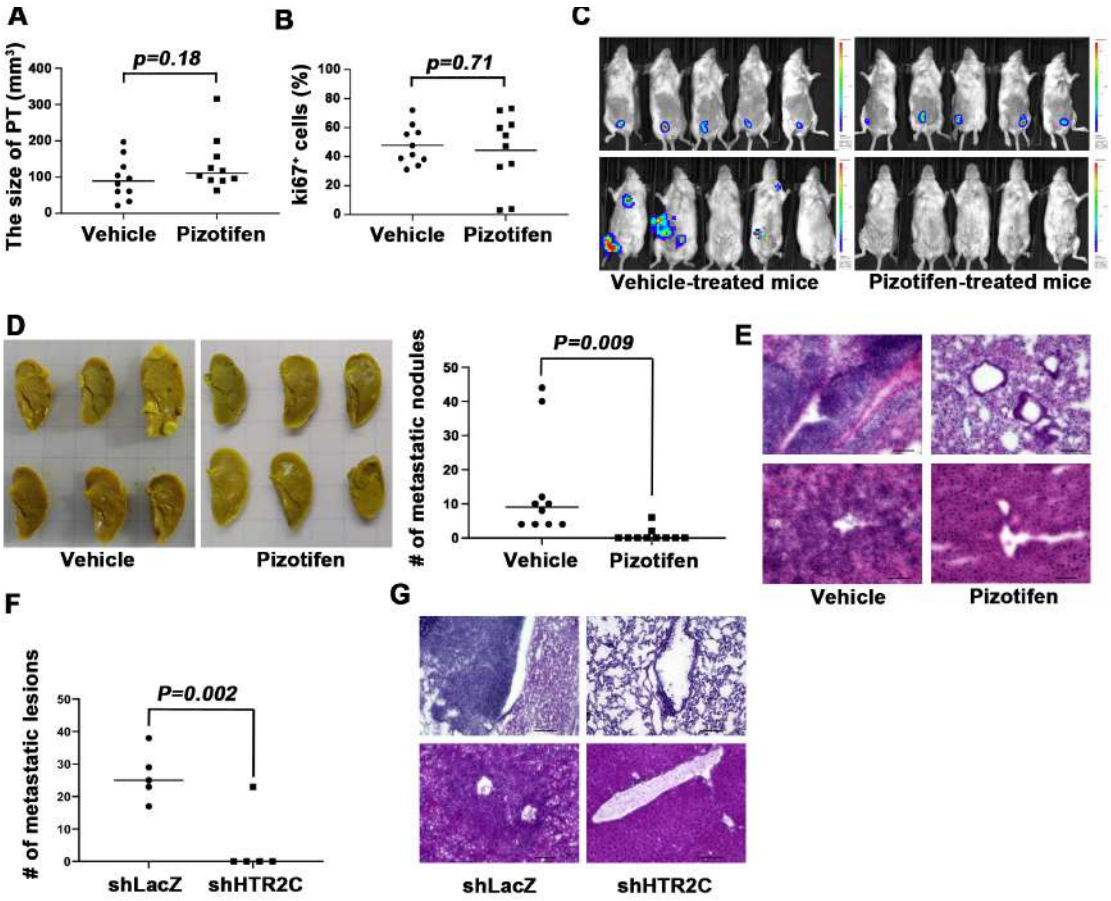

Figure 3. Pizotifen suppressed metastatic progression in a mouse model of metastasis.

(A) Mean volumes (n=10 per group) of 4T1 primary tumors formed in the mammary fat pad of either vehicle or Pizotifen-treated mice at day 10 post injection. (B) Ki67 expression level in 4T1 primary tumors formed in the mammary fat pad of either vehicle or Pizotifen-treated mice at day 10 post injection. The mean expression levels of Ki67 (n=10 mice per group) were determined and were calculated as the mean ration of Ki67 positive cells to DAPI area. (C) Representative images of primary tumors on day 10 post injection (top panels) and metastatic burden on day 70 post injection (bottom panels) taken using an IVIS Imaging System. (D) Representative images of the lungs from either vehicle (top) or Pizotifen-treated mice (bottom) at 70 days past tumor inoculation.

Number of metastatic nodules in the lung of either vehicle or Pizotifen-treated mice (right). (E) Representative H&E staining of the lung (top) and liver (bottom) from either vehicle or Pizotifen-treated mice. (F) The mean number of metastatic lesions in step sections of the lungs from the mice that were inoculated with 4T1-12B cells expressing shRNA targeting for either LacZ or HTR2C. (G) Representative H&E staining of the lung and liver from the mice that were inoculated with 4T1-12B cells expressing shRNA targeting for either LacZ or HTR2C. Each value is indicated as the mean ± SEM. Statistical analysis was determined by Student's *t* test.

390 **Figure 4**

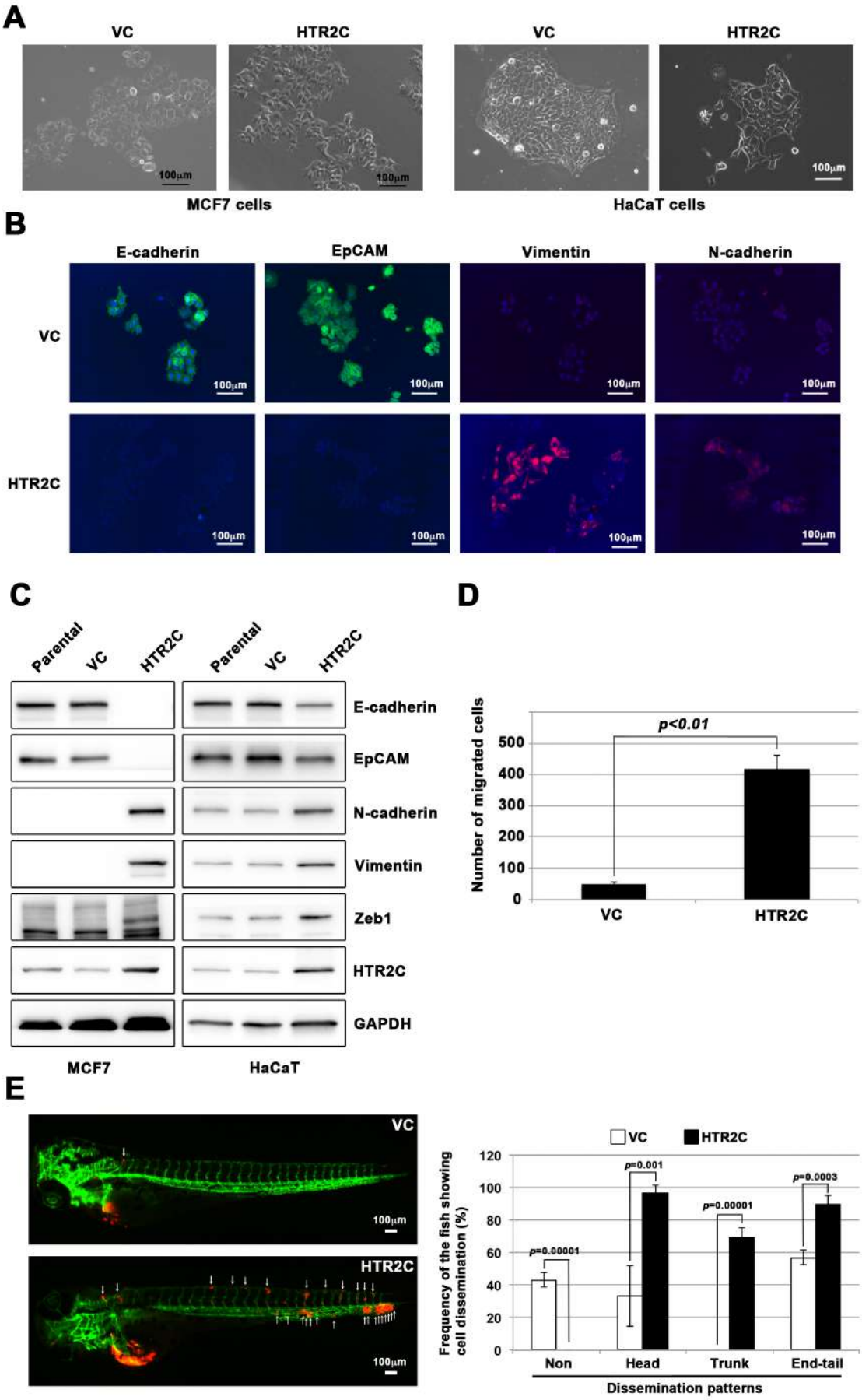

391

Figure 4. HTR2C induced EMT-mediated metastatic dissemination of human cancer cells.

(A) The morphologies of the MCF7 and HaCaT cells expressing either the control vector or HTR2C were revealed by phase contrast microscopy. (B) Immunofluorescence staining of E-cadherin, EpCAM, Vimentin, and N-cadherin expressions in the MCF7 cells from Figure 4A. (C) Expression of E-cadherin, EpCAM, Vimentin, N-cadherin, and HTR2C was examined by western-blotting in the MCF7 and HaCaT cells; GAPDH loading control is shown (bottom). (D) Effect of HTR2C on cell motility and invasion of MCF7 cells. MCF7 cells were subjected to Boyden chamber assays. Fetal bovine serum (1%v/v) was used as the chemoattractant in both assays. Each experiment was performed at least twice. (E) Representative images of dissemination patterns of MCF7 cells expressing either the control vector (top left) or HTR2C (lower left) in a zebrafish xenotransplantation model. White arrows head indicate disseminated MCF7 cells. The mean frequencies of the fish showing head, trunk, or end-tail dissemination tabulated (right). Each value is indicated as the mean ± SEM of two independent experiments. Statistical analysis was determined by Student's *t* test.

See also Table S6.

409 **Figure 5**

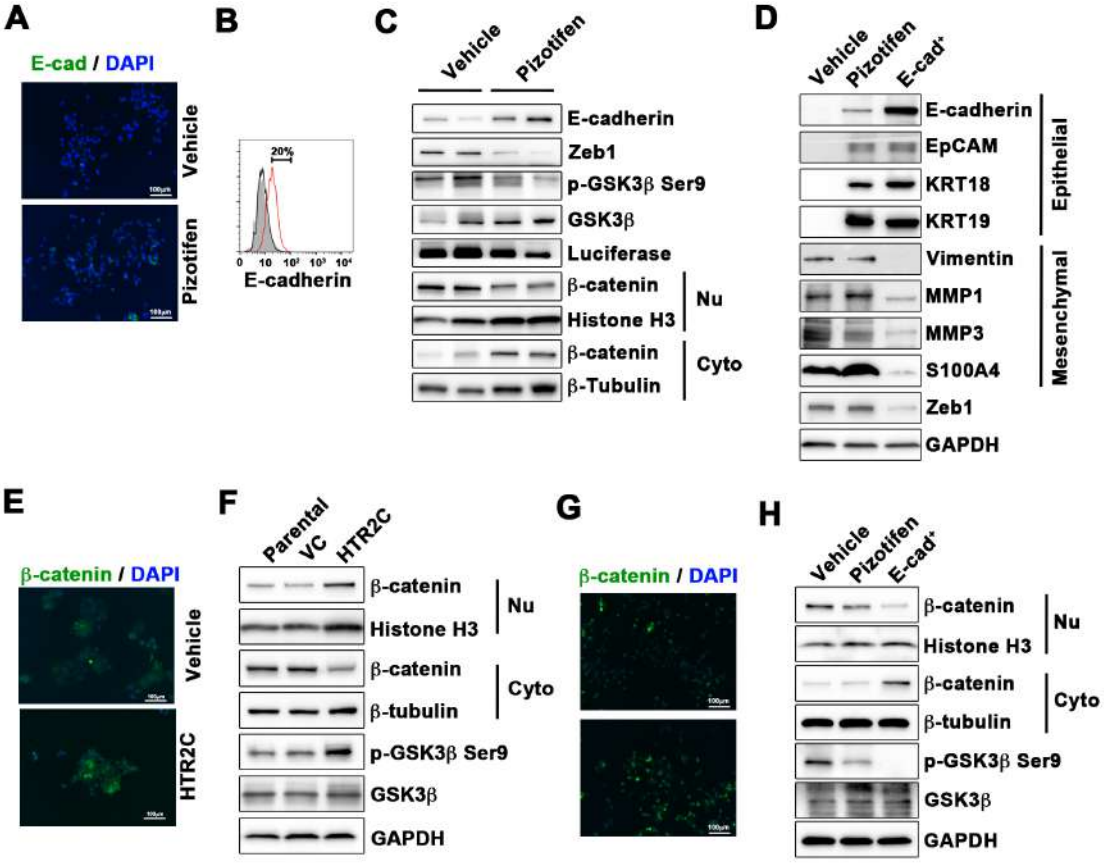

410

411 **Figure 5. Pizotifen restored mesenchymal-like traits of MDA-MB-231 cells into**

412 **epithelial traits through blocking nuclear accumulation of β-catenin.**

413 (A) IF staining of E-cadherin in either vehicle or Pizotifen-treated MDA-MB-231 cells.

414 (B) Surface expression of E-cadherin in either vehicle (black) or Pizotifen (red)-treated

415 MDA-MB-231 cells by FACS analysis. Non-stained controls are shown in gray. (C)

416 Protein expressions levels of E-cadherin, Zeb1, and β-catenin in the cytoplasm and

417 nucleus of 4T1 primary tumors from either vehicle or Pizotifen-treated mice are shown;

418 Luciferase, Histone H3, and β-tubulin are used as loading control for whole cell, nuclear

419 or cytoplasmic lysate, respectively. (D) Protein expression levels of epithelial and

420 mesenchymal markers and Zeb1 in either vehicle or Pizotifen-treated MDA-MB-231 cells

421 or E-cadherin positive (E-cad^{+}) cells in Pizotifen-treated MDA-MB-231 cells are shown.

422 (E) Immunofluorescence staining of β-catenin in the MCF7 cells expressing either vector

423 control or HTR2C. (F) Expressions of β-catenin in the cytoplasm and nucleus of MCF7

424 cells. (G) IF staining of β-catenin in either vehicle or Pizotifen-treated MDA-MB-231

425 cells. (H) Expressions of β-catenin in the cytoplasm and nucleus of MDA-MB-231 cells

426 and the E-cad^{+} cells.

427

Table 1. Primary targets of the identified drugs

The identified drugs	Primary targets of the identified drugs
Hexachlorophene	D-lactate dehydrogenase (D-LDH), not expressed in mammalian cells
Troglitazone	Agonist for Peroxisome proliferator-activated receptor α and γ (PPARα and γ)
Pizotifen malate	5-hydroxytryptamine receptor 2C (HTR2C)
Salmeterol	Adrenergic receptor beta 2 (ADRB2)
Nitazoxanide	Pyruvate ferredoxin oxidoreductase (PFOR), not expressed in mammalian cells
Valproic acid	Histone deacetylases (HDACs)
Dicumarol	NAD(P)H dehydrogenase quinone 1 (NQO1)
Loxapine succinate	Dopamine receptor D2 and D4 (DRD2 and DRD4)
Adrenosterone	Hydroxysteroid (11-beta) dehydrogenase 1 (HSD11β1)
Riluzole hydrochloride	Glutamate R and Voltage-dependent Na+ channel
Naftopidil dihydrochloride	5-hydroxytryptamine receptor 1A (HTR1A) and α1-adrenergic receptor (AR)
S(-)Eticlopride hydrochloride	Dopamine receptor D2 (DRD2)
Racecadotril	Membrane metallo-endopeptidase (MME)
Ipriflavone	Unknow
Flurbiprofen	Cyclooxygenase 1 and 2 (Cox1 and 2)
Zardaverine	Phosphodiesterase III/IV (PDE3/4)
Leflunomide	Dihydroorotate dehydrogenase (DHODH)
Olmesartan	Angiotensin II receptor alpha
Disulfiram	Aldehyde dehydrogenase (ALDH) Dopamine β-hydroxylase (DBH)
Zuclopenthixol dihydrochloride	Dopamine receptors D1 and D2 (DRD1 and 2)

Discussion

Reducing or eliminating mortality associated with metastatic disease is a key goal of medical oncology, but few models exist that allow for rapid, effective screening of novel compounds that target the metastatic dissemination of cancer cells. Based on accumulated

evidence that at least fifty genes play an essential role in governing both metastasis and gastrulation progression (Table 1S), we hypothesized that small molecule inhibitors that interrupt gastrulation of zebrafish embryos might suppress metastatic progression of human cancer cells. We created a unique screening concept utilizing gastrulation of zebrafish embryos to test the hypothesis. Our results clearly confirmed our hypothesis: 25.6% (20/76 drugs) of epiboly-interrupting drugs could also suppress cell motility and invasion of highly metastatic human cell lines in vitro. In particular, Pizotifen which is an antagonist for serotonin receptor 2C and one of the epiboly-interrupting drugs, could suppress metastasis in a mouse model (Figure 3A-E). Thus, this screen could offer a novel platform for discovery of anti-metastasis drugs.

There are at least two advantages to the screen described herein. One is that the screen can easily be converted to a chemical genetic screening platform. Indeed, we have provided the first evidence that HTR2C, which is a primary target of Pizotifen, induced EMT and promoted metastatic dissemination of cancer cells (Figure 4A-E). In this research, 1,280 FDA approval drugs were screened, this is less than a few percent of all of druggable targets (approximately 100 targets) in the human proteome in the body. If chemical genetic screening using specific inhibitor libraries were conducted, more genes that contribute to metastasis and gastrulation could be identified. The second advantage is that the screen enables one researcher to test 100 drugs in 5 hours with using optical microscopy, drugs, and zebrafish embryos. That indicates this screen is not only highly efficient, low-cost, and low-labor but also enables researchers who do not have high throughput screening instruments to conduct drug screening for anti-metastasis drugs.

Acknowledgments

We sincerely appreciate Dr. Joshua Collins (NIH/NIDCR) and Dr. Diane Palmieri (NIH/NCI) for helping this research. We thank Dr. Herrick (Albany medical collage) for providing pCMV-h5TH2C-VSV with us. This study was funded by grants from National

Medical Research Council of Singapore (R-154000547511) and Ministry of Education of Singapore (R-154000A23112) to Z.G.

Author Contributions

Design research; J.N. Conducting experiments; J.N. and L.T. Analyzing data: J.N. Writing the paper; J.N. and Z.G. Funding Acquisition; Z.G, S.W. B.C.G., H.M. and Supervision; Z.G.

Declaration of Interests

J.N., L.T., B.C.G., S.W., H.M. and G.Z. declare no conflict of interest.

Materials and Methods

Zebrafish embryo screening

Zebrafish embryos at two cell stage were collected at 20 mins after their fertilization. Each drug was added to a well of a 24-well plate containing approximately 20 zebrafish embryos per well in either 10 μM or 50 μM final concentration when the embryos reached the sphere stage. Chemical treatment was initiated at 4 hours post-fertilization (hpf) and approximately 20 embryos were treated with two different concentrations for each compound tested. The treatment was ended at 9 hpf when vehicle (DMSO) treated embryos as control reach 80-90% completion of the epiboly stage. The compounds which induced delay (<50% epiboly) in epiboly were selected as hit compounds for in vitro testing using highly metastatic human cancer cell lines. The study protocol was approved by the Institutional Animal Care and Use Committee of the National University of Singapore (protocol number: R16-1068).

Reagents

FDA, EMA and other agencies approved chemical libraries was purchased from Prestwick Chemical (Illkirch, France). Pizotifen and S(-) Eticlopride hydrochloride were purchased from Sigma-Aldrich (St. Louis, MO).

Cell culture and cell viability assay

MCF7, MDA-MB-231, MDA-MB-435, MIA-PaCa2, PC3, SW620, PC9 and HaCaT cells were obtained from American Type Culture Collection (ATCC, Manassas, VA). Luciferase-expressing 4T1 (4T1-12B) cells were provided from Dr. Gary Sahagian (Tufts University, Boston, MA). All culture methods followed the supplier's instruction. Cell viability assay was performed as previously described (16).

Plasmid

A DNA fragment coding for HTR2C was amplified by PCR with primers containing restriction enzyme recognition sequences. The HTR2C coding fragment was amplified from hsp70l:mCherry-T2A-CreERT2 plasmid (17).

Immunoblotting

Western blotting was performed as described previously (16). Anti-PRMT1, anti-CYP11A1, anti-E-cadherin, anti-EpCAM, anti-Vimentin, anti-N-cadherin, anti-Zeb1, anti-Histone H_3, anti-α-tubulin and anti-GAPDH antibodies were purchased from Cell signaling Technology. Anti-HTR2C and anti-DRD2 antibodies were purchased form Abcam. Anti-phospho-GSK3β (Ser9), anti-GSK3β, Anti-KRT18, anti-KRT19, anti-MMP1, anti-MMP2, anti-S100A4, anti-Luciferase, and anti-β-catenin antibodies were purchased from Santa Cruz.

Flow cytometry

Cells were stained with FITC-conjugated E-cadherin antibody (Biolegend, San Diego, CA). Flow cytometry was performed as described (26) and analyzed with FlowJo software (TreeStar, Ashland, OR).

shRNA mediated gene knockdown

The short hairpin RNA (shRNA)-expressing lentivirus vectors were constructed using pLVX-shRNA1 vector (Clontech). PRMT1-shRNA_#3–targeting sequence is GTGTTCCAGTATCTCTGATTA; PRMT1-shRNA_#4–targeting sequence is TTGACTCCTACGCACACTTTG. CYP11A1-shRNA_#4–targeting sequence is GCGATTCATTGATGCCATCTA; CYP11A1-shRNA_#4–targeting sequence is GAAATCCAACACCTCAGCGAT. Human HTR2C-shRNA–targeting sequence is TCATGCACCTCTGCGCTATAT. Mouse HTR2C-shRNA–targeting sequence is CTTCATACCGCTGACGATTAT. LacZ-shRNA– targeting sequence is CTACACAAATCAGCGATT.

Immunofluorescence

Immunofluorescence microscopy assay was performed by previously described (16). Goat anti-mouse and goat anti-rabbit immunoglobulin G (IgG) antibodies conjugated to Alexa Fluor 488 (Life Technologies) and diluted at 1:100 were used. Nuclei were visualized by the addition of 2μg/ml of 4', 6-diamidino-2-phenylindole (DAPI) and photographed at 100x magnification by a fluorescent microscope BZ-X700 (KEYENCE, Japan).

Boyden chamber cell motility and invasion assay

These assays were performed by previously described (16). In Boyden chamber assay, either $3x10^5$ MDA-MB-231, $1x10^6$ MDA-MB-435, or $5x10^5$ PC9 cells were applied to each well in the upper chamber.

Zebrafish xenotransplantation model

Tg(kdrl:eGFP) zebrafish was provided by Dr. Stainier (Max Planck Institute for Heart and Lung Research). Embryos that were derived from the line were maintained in E3 medium containing 200μM 1-phenyl-2-thiourea (PTU). Approximately 100-400 Red fluorescence protein (RFP)-labelled MBA-MB-231 or MIA-Paca2 cells were injected into the duct of Cuvier of the zebrafish at 2dpf. The fish were randomly assigned to two groups. One group was maintained in the presence of pizotifen-containing E3 medium and the other group was maintained in vehicle-containing E3 medium.

Spontaneous metastasis mouse model

4T1-12B cells ($2x10^4$) were injected into the #4 mammary fat pad while the mice were anesthetized. To monitor tumor growth and metastases, mice were imaged biweekly by IVIS Imaging System (ParkinElmer). The primary tumor was resected 10 days after inoculation. The study protocol (protocol number: BRC IACUC #110612) was approved by A*STAR (Agency for Science, Technology and Research, Singapore).

Histological Analysis

All OCT embedded primary tumors, lungs, and livers of mice from the spontaneous metastasis 4T1 model were sectioned on a cryostat. Eight micron sections were taken at five hundred micron intervals through the entirety of the livers and lungs. Sections were subsequently stained with hematoxylin and eosin. Metastatic lesions were counted under a microscope in each section for both lungs and livers.

Statistics

Data were analyzed by Student's t test; $p < 0.05$ was considered significant.

References

1. Chambers AF, Groom AC, & MacDonald IC (2002) Dissemination and growth of cancer cells in metastatic sites. *Nature reviews. Cancer* 2(8):563-572.
2. Steeg PS (2003) Metastasis suppressors alter the signal transduction of cancer cells. *Nature reviews. Cancer* 3(1):55-63.
3. Fidler IJ (2003) The pathogenesis of cancer metastasis: the 'seed and soil' hypothesis revisited. *Nature reviews. Cancer* 3(6):453-458.
4. Cavallaro U & Christofori G (2004) Cell adhesion and signalling by cadherins and Ig-CAMs in cancer. *Nature reviews. Cancer* 4(2):118-132.
5. Ellenbroek SI, Iden S, & Collard JG (2012) Cell polarity proteins and cancer. *Semin Cancer Biol* 22(3):208-215.
6. Tsai JH & Yang J (2013) Epithelial-mesenchymal plasticity in carcinoma metastasis. *Genes & development* 27(20):2192-2206.
7. Solnica-Krezel L (2005) Conserved patterns of cell movements during vertebrate gastrulation. *Curr Biol* 15(6):R213-228.
8. Latimer A & Jessen JR (2010) Extracellular matrix assembly and organization during zebrafish gastrulation. *Matrix Biol* 29(2):89-96.
9. Solnica-Krezel L (2006) Gastrulation in zebrafish -- all just about adhesion? *Curr Opin Genet Dev* 16(4):433-441.
10. Tsai YJ, *et al.* (2011) The predominant protein arginine methyltransferase PRMT1 is critical for zebrafish convergence and extension during gastrulation. *FEBS J* 278(6):905-917.
11. Hsu HJ, Liang MR, Chen CT, & Chung BC (2006) Pregnenolone stabilizes microtubules and promotes zebrafish embryonic cell movement. *Nature* 439(7075):480-483.
12. Weinbach EC & Garbus J (1969) Mechanism of Action of Reagents that uncouple Oxidative Phosphorylation. *Nature* 221:1016.
13. Sack U, *et al.* (2011) Novel effect of antihelminthic Niclosamide on S100A4-mediated metastatic progression in colon cancer. *Journal of the National Cancer Institute* 103(13):1018-1036.
14. Huang EW, *et al.* (2012) Vinpocetine inhibits breast cancer cells growth in vitro and in vivo. *Apoptosis : an international journal on programmed cell death* 17(10):1120-1130.
15. Szilágyi G, *et al.* (2005) Effects of vinpocetine on the redistribution of cerebral blood flow and glucose metabolism in chronic ischemic stroke patients: a PET study. *Journal of the Neurological Sciences* 229-230:275-284.
16. Nakayama J, Lu J, Makinoshima H, & Gong Z (2020) A Novel Zebrafish Model of Metastasis Identifies the HSD11β1 Inhibitor Adrenosterone as a Suppressor of Epithelial-Mesenchymal Transition and Metastatic Dissemination. *Mol Cancer Res* 18(3):477-487.
17. Kolosionek E, *et al.* (2009) Expression and activity of phosphodiesterase isoforms during epithelial mesenchymal transition: the role of phosphodiesterase 4. *Mol Biol Cell* 20(22):4751-4765.
18. Sasaki T, *et al.* (2014) Serum CD10 is associated with liver metastasis in colorectal cancer. *J Surg Res.* 192(2):390-394.
19. Liu P, *et al.* (2013) Disulfiram targets cancer stem-like cells and reverses resistance and cross-resistance in acquired paclitaxel-resistant triple-negative breast cancer cells. *British journal of cancer* 109(7):1876-1885.
20. Gunnarsson L, Jauhiainen A, Kristiansson E, Nerman O, & Larsson DGJ (2008) Evolutionary conservation of human drug targets in organisms used for environmental risk assessments. *Environmental Science & Technology* 42(15):5807-5813.
21. Tao K, Fang M, Alroy J, & Sahagian GG (2008) Imagable 4T1 model for the study of late stage breast cancer. *BMC cancer* 8:228.

22. Kröger C, Afeyan, A.; Mraz, J.; Eaton, EN.; Reinhardt, F.; Khodor, YL.; Thiru, P.; Bierie B.; Ye, X.; Burge, CB.; Weinberg RA (2019) Acquisition of a hybrid E/M state is essential for tumorigenicity of basal breast cancer cells. *Proceedings of the National Academy of Sciences of the United States of America* 116(15):7353-7362.
23. Beyer TD, M.; Thumberger, T.; Vick, P.; Tisler, M.; Schneider, I.; Bogusch, S.; Andre, P.; Ulmer, B.; Walentek, P.; Niesler, B.; Blum, M.; Schweickert, A. (2012) Serotonin signaling is required for Wnt-dependent GRP specification and leftward flow in Xenopus. *Curr Biol* 22(1):33-39.
24. Sui HX, H.; Ji, Q.; Liu, X.; Zhou, L.; Song, H.; Zhou, X.; Xu, Y.; Chen, Z.; Cai, J.; Ji, G.; Li, Q. (2015) 5-hydroxytryptamine receptor (5-HT1DR) promotes colorectal cancer metastasis by regulating Axin1/β-catenin/MMP-7 signaling pathway. *Oncotarget* 6(28):25975-25987.
25. Zhan TR, N.; Boutros, M. (2017) Wnt signaling in cancer. *Oncogene* 36(11):1461–1473.
26. Nakayama J*, et al.* (2009) BLNK suppresses pre-B-cell leukemogenesis through inhibition of JAK3. *Blood* 113(7):1483-1492.

Supplemental Information

Figure S1.

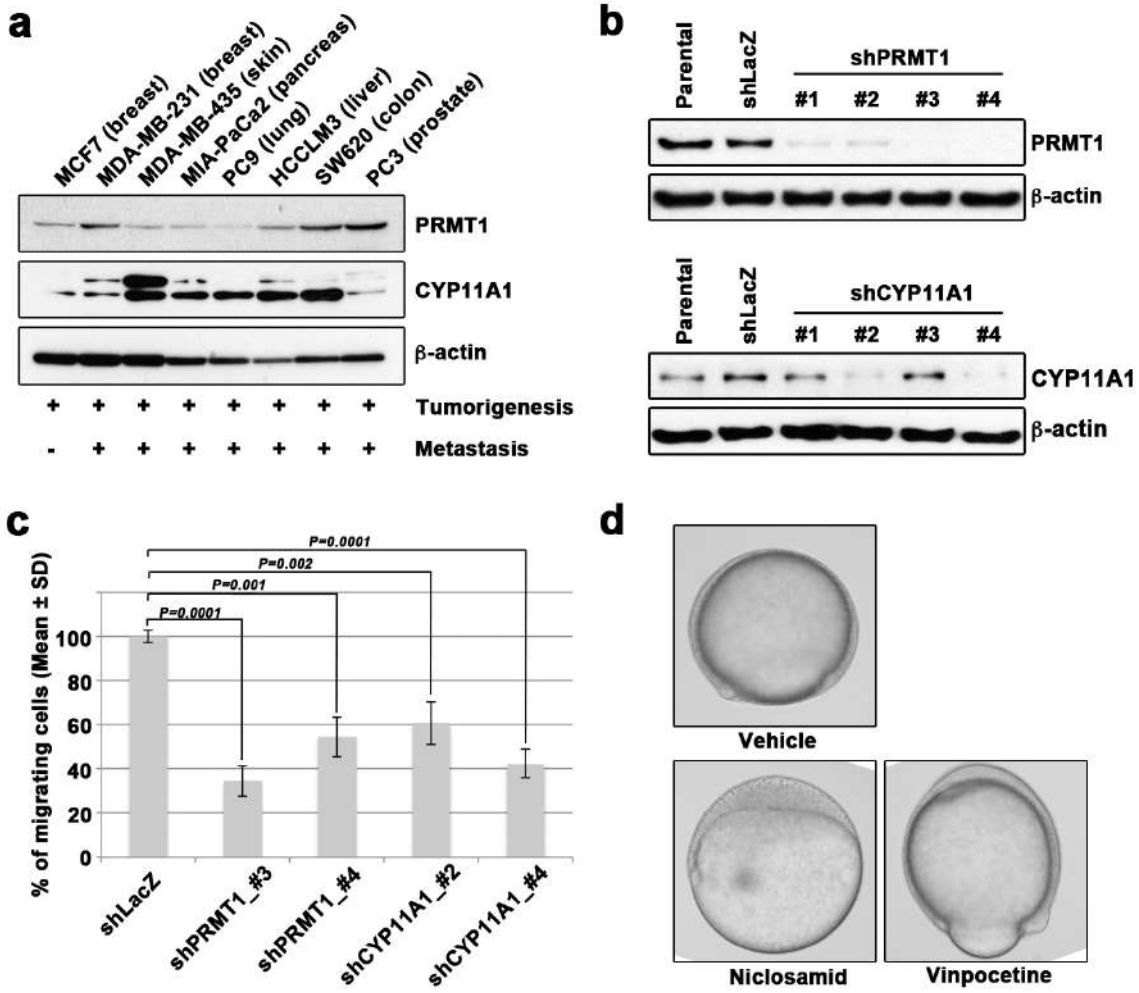

Figure S1. Molecular mechanisms of epiboly in zebrafish overlap with those in cancer metastasis.

(A) Western blot analysis of PRMT1 (upper) and CYP11A1 (middle) protein levels in non-metastatic human cancer cell line (MCF7) and highly metastatic human cancer cell lines (MDA-MB-231, MDA-MB-435, MIA-PaCa2, PC9, HCCLM3, PC3 and SW620); β-actin loading control is shown (bottom). (B) Knockdown of PRMT1 or CYP11A1 in MDA-MB-231 cells. MBA-MB-231 cells were transfected with a control shRNA targeting LacZ, and one of four independent shRNAs targeting PRMT1 (clone #1 to #4) or one of two independent shRNAs targeting CYP11A1 (clone #1 to #4). Reduced PRMT1 and CYP11A1 expression, determined by western blot, in sub-cell lines of

MDA-MB-231 cells expressing PRMT1 shRNA (clone #3 and #4 or CYP11A1 (clone #2 and #4), compared with controls (parental cell line MDA-MB-231 and control shRNA cells); β-actin levels shown as a loading control. (C) Effect of shRNAs targeting either PRMT1 or CYP11A1 on cell motility and invasion of MBA-MB-231 cells. Parental MDA-MB-231 cells and four sub-cell lines of MDA-MB-231 cells that were transfected with either shRNA targeting either LacZ, two independent shRNAs targeting PRMT1 (clone #3 and #4) or two independent shRNAs targeting CYP11A1 (clone #2 and #4), were subjected to Boyden chamber assays. (D) Zebrafish embryos treated with either vehicle (DMSO), 10μM Niclosamide, or 50μM vinpocetine. Approximately 20 embryos were treated with either DMSO as a vehicle control, niclosamide, or vinpocetine. The treatment was started at 4 hpf when all of embryos reached sphere stage and ended at 9 hpf when control embryos reached 80-90% epiboly stage. Each experiment was performed at least twice. Statistical analysis was determined by Student's *t* test.

Figure S2.

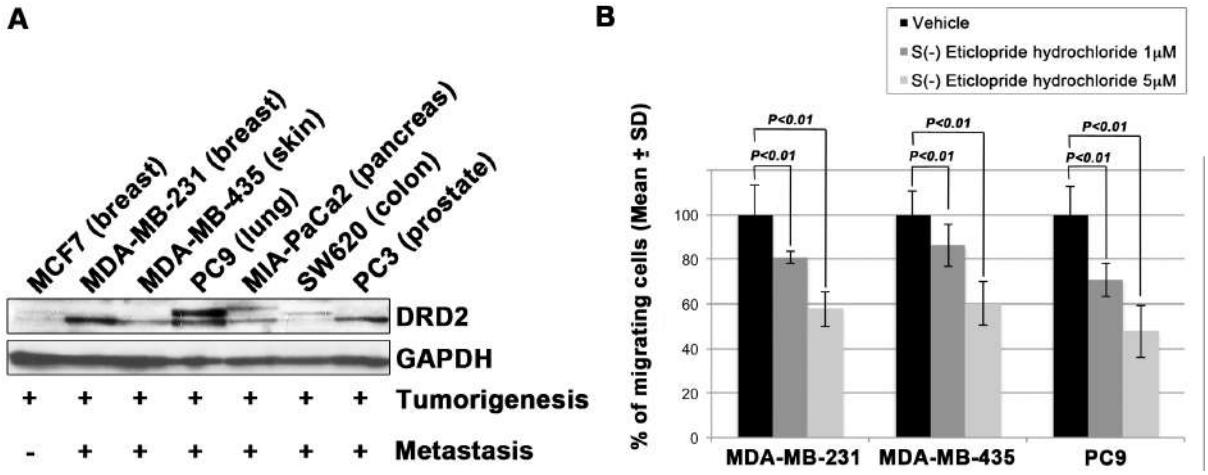

Figure S2. S (-) Eticlopride hydrochloride suppressed cell motility and invasion of human cancer cells.

Related to Figure 2.

(A) Western blot analysis of DRD2 levels in non-metastatic human cancer cell line, MCF7 (breast) and highly metastatic human cancer cell lines, MDA-MB-231 (breast), MDA-MB-435 (melanoma), MIA-PaCa2 (pancreas), PC3 (prostate) and SW620 (colon); GAPDH loading control is shown (bottom). (B) Effect of S (-) Eticlopride hydrochloride on cell motility and invasion of MBA-MB-231, MDA-MB-435, and PC9 cells. Either vehicle or pizotifen treated cells were subjected to Boyden chamber assays. Fetal bovine serum (1%v/v) was used as the chemoattractant in both assays. Each experiment was performed at least twice. Statistical analysis was determined by Student's *t* test.

688 **Figure S3.**

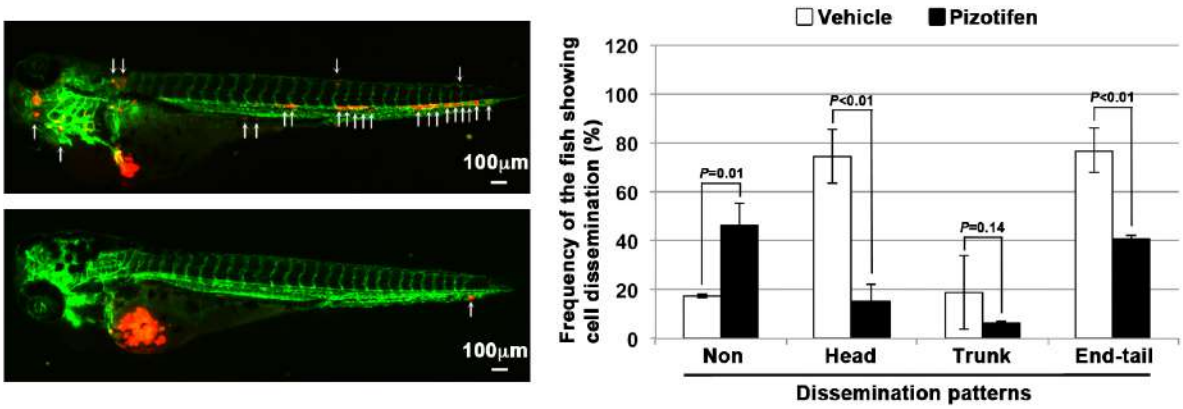

689

690 **Figure S3. Pizotifen suppressed metastatic dissemination of human pancreatic**

691 **cancer cells in a zebrafish xenotransplantation model.**

692 Related to Figure 2.

693 Representative images of dissemination of MIA-PaCa2 cells in zebrafish

694 xenotransplantation model. The fish were inoculated with MIA-PaCa2 cells, and treated

695 with either vehicle (top left) or drug (lower left). White arrows heads indicate

696 disseminated MIA-PaCa2 cells. The images were shown in 4x magnification. Scale bar,

697 100μm. The mean frequencies of the fish showing head, trunk, or end-tail dissemination

698 were tabulated (right). Each value is indicated as the mean ± SEM of two independent

699 experiments. Statistical analysis was determined by Student's *t* test.

700

Table S1. A list of the genes that are involved between gastrulation and metastasis progression

Genes	Gastrulation Defects	Ref	Effects in Metastasis	Ref
BMP	Convergence and extension	(1)	EMT	(2)
WNT	Convergence and extension	(3)	Migration and Invasion	(4)
FGF	Convergence and extension	(5)	Invision	(6)
EGF	Epiboly	(7)	Migration	(8)
PDGF	Convergence and extension	(9)	EMT	(10)
CXCL12	Migration of endodermal cells	(11)	Migration and Invasion	(12)
CXCR4	Migration of endodermal cells	(11)	Migration and Invasion	(12)
PIK3CA	Convergence and extension	(13)	Migration and Invasion	(14)
YES	Epiboly	(15)	Migration	(16)
FYN	Epiboly	(17)	Migration and Invasion	(18)
MAPK1	Epiboly	(19)	Migration	(20)
SHP2	Convergence and extension	(21)	Migration	(22)
SNAI1	Convergence and extension	(23)	EMT	(24)
SNAI2	Mesoderm & Neural crest formation	(25)	EMT	(95)
TWIST1	Mesoderm formation	(26)	EMT	(27)
TBXT	Convergence and extension	(3)	EMT	(28)
ZEB1	Epiboly	(29)	EMT	(30)
GSC	Mesodermal patterning	(31)	EMT	(32)
FOXC2	Unclear, defects in gastrulation	(33)	EMT	(34)
STAT3	Convergence and extension	(35)	Migration	(36)
POU5F1	Epiboly	(37)	EMT	(38)
EZH2	Unclear, defects in gastrulation	(39)	Invasion	(40)
EHMT2	Defects in Neurogenesis	(41)	Migration and Invasion	(42)
BMI1	Defects in skelton formation	(43)	EMT	(44)
RHOA	Convergence and extension	(45)	Migration and Invasion	(46)
CDC42	Convergence and extension	(47)	Migration and Invasion	(48)
RAC1	Convergence and extension	(49)	Migration and Invasion	(50)
ROCK2	Convergence and extension	(51)	Migration and Invasion	(52)
PAR1	Convergence and extension	(53)	Migration	(54)
PRKCI	Convergence and extension	(53)	EMT	(55)
CAP1	Convergence and extension	(56)	Migration	(57)
EZR	Epiboly	(58)	Migration	(59)
EPCAM	Epiboly	(60)	Migration and Invasion	(61)
ITGB1 / ITA5	Mesodermal Migration	(62)	Migration and Invasion	(63)
FN1	Convergence and extension	(64)	Invasion	(65)
HAS2	Dorsal migration of lateral cells	(66)	Invasion	(67)
MMP14	Convergence and extension	(68)	Invasion	(69)
COX1	Epiboly	(70)	Invasion	(71)
PTGES	Convergence and extension	(72)	Invasion	(73)
SLC39A6	Aterior migration	(74)	EMT	(75)
GNA12 / 13	Convergence and extension	(41)	Migration and Invasion	(76)
OGT	Epiboly	(77)	Migration and Invasion	(78)
CCN1	Cell Movement	(79)	Migration and Invasion	(80)
TRPM7	Convergence and extension	(81)	Migration	(82)
MAPKAPK2	Epiboly	(83)	Migration	(84)
B4GALT1	Convergence and extension	(85)	Invasion	(86)
IER2	Convergence and extension	(87)	Migration	(88)
TIP1	Convergence and extension	(89)	Migration and Invasion	(90)
PAK5	Convergence and extension	(91)	Migration	(92)
MARCKS	Convergence and extension	(93)	Migration and Invasion	(94)

Table S1.

A list of the fifty genes that play essential role in governing both metastasis and gastrulation progression. The gastrulation defects in Xenopus or zebrafish that are induced by knockdown of each of these genes, were indicated. The molecular

709 mechanism in metastasis that are inhibited by knockdown of each of the same genes,

710 were indicated.

711 **Table S2. A list of the drugs that interfere with epiboly progression in zebrafish**
712

Chemical name	Chemical formula	Effect of 10uM	Effect of 50uM
Acitretin	C21H26O3	Delayed	Delayed
Adrenosterone	C19H24O3	Delayed	Delayed
Albendazole	C12H15N3O2S	Severe delayed	Severe delayed
Alfadolone acetate	C23H34O5	Delayed	Delayed
Alfaxalone	C21H32O3	Delayed	Delayed
Alprostadil	C20H34O5	Delayed	Delayed
Altrenogest	C21H26O2	Slightly delayed	Delayed
Ampiroxicam	C20H21N3O7S	Non effect	Delayed
Anethole-trithione	C10H8OS3	Delayed	Delayed
Antimycin A	C28H40N2O9	Delayed	Delayed
Avobenzone	C20H22O3	Delayed	Delayed
Benzoxiquine	C16H11NO2	Non effect	Delayed
Bosentan	C27H29N5O6S	Delayed	Delayed
Butoconazole nitrate	C19H18Cl3N3O3S	Delayed	Toxic lethal
Camptothecine (S,+)	C20H16N2O4	Severe delayed	Severe delayed
Carbenoxolone disodium salt	C34H48Na2O7	Delayed	Toxic lethal
Carmofur	C11H16FN3O3	Slightly delayed	Delayed
Carprofen	C15H12ClNO2	Severe delayed	Toxic lethal
Cefdinir	C14H13N5O5S2	Delayed	Delayed
Celecoxib	C17H14F3N3O2S	Delayed	Delayed
Chlorambucil	C14H19Cl2NO2	Slightly delayed	Delayed
Chlorhexidine	C22H30Cl2N10	Non effect	Toxic lethal
Ciclopirox ethanolamine	C14H24N2O3	Delayed	Severe delayed
Cinoxacin	C12H10N2O5	Delayed	Severe delayed
Clofibrate	C12H15ClO3	Non effect	Severe delayed
Clopidogrel	C16H16ClNO2S	Non effect	Delayed
Clorgyline hydrochloride	C13H16Cl3NO	Delayed	Delayed
Colchicine	C22H25NO6	Non effect	Delayed
Deptropine citrate	C29H35NO8	Delayed	Delayed
Desipramine hydrochloride	C18H23ClN2	Delayed	Delayed
Diclofenac sodium	C14H10Cl2NNaO2	Delayed	Severe delayed
Dicumarol	C19H12O6	Delayed	Severe delayed
Diethylstilbestrol	C18H20O2	Delayed	Toxic lethal
Dimaprit dihydrochloride	C6H17Cl2N3S	Slightly delayed	Delayed
Disulfiram	C10H20N2S4	Delayed	Delayed
Dopamine hydrochloride	C8H12ClNO2	Delayed	Delayed
Eburnamonine (-)	C19H22N2O	Delayed	Delayed
Ethaverine hydrochloride	C24H30ClNO4	Delayed	Delayed
Ethinylestradiol	C20H24O2	Delayed	Severe delayed
Ethopropazine hydrochloride	C19H25ClN2S	Delayed	Delayed
Ethoxyquin	C14H19NO	Non effect	Delayed
Exemestane	C20H24O2	Slightly delayed	Delayed
Ezetimibe	C24H21F2NO3	Slightly delayed	Delayed
Fenbendazole	C15H13N3O2S	Non effect	Delayed
Fenoprofen calcium salt dihydrate	C30H30CaO8	Slightly delayed	Delayed
Fentiazac	C17H12ClNO2S	Toxic lethal	Toxic lethal
Floxuridine	C9H11FN2O5	Delayed	Toxic lethal
Flunixin meglumine	C21H28F3N3O7	Delayed	Toxic lethal
Flutamide	C11H11F3N2O3	Delayed	Toxic lethal
Fluticasone propionate	C25H31F3O5S	Non effect	Delayed
Furosemide	C12H11ClN2O5S	Delayed	Delayed
Gatifloxacin	C19H22FN3O4	Delayed	Delayed
Gemcitabine	C9H11F2N3O4	Delayed	Delayed
Gemfibrozil	C15H22O3	Delayed	Toxic lethal
Gestrinone	C21H24O2	Delayed	Delayed
Haloprogin	C9H4Cl3IO	Delayed	Toxic lethal
Hexachlorophene	C13H6Cl6O2	Delayed	Severe delayed
Hexestrol	C18H22O2	Slightly delayed	Delayed
Ibudilast	C14H18N2O	Non effect	Delayed
Idazoxan hydrochloride	C11H13ClN2O2	Slightly delayed	Delayed
Idazoxan hydrochloride	C11H13ClN2O2	Non effect	Delayed

Idebenone	C19H30O5	Severe delayed	Toxic lethal
Indomethacin	C19H16ClNO4	Non effect	Delayed
Ipriflavone	C18H16O3	Delayed	Severe delayed
Isotretinoin	C20H28O2	Non effect	Severe delayed
Isradipine	C19H21N3O5	Non effect	Delayed
Lansoprazole	C16H14F3N3O2S	Slightly delayed	Delayed
Latanoprost	C26H40O5	Non effect	Delayed
Leflunomide	C12H9F3N2O2	Delayed	Severe delayed
Letrozole	C17H11N5	Non effect	Delayed
Lithocholic acid	C24H40O3	Non effect	Delayed
Lodoxamide	C11H6ClN3O6	Non effect	Delayed
Lofepramine	C26H27ClN2O	Non effect	Delayed
Loratadine	C22H23ClN2O2	Delayed	Delayed
Loxapine succinate	C22H24ClN3O5	Delayed	Delayed
Mebendazole	C16H13N3O3	Severe delayed	Severe delayed
Mebendazole	C22H26N2O2	Non effect	Delayed
Meloxicam	C14H13N3O4S2	Delayed	Toxic lethal
Methiazole	C12H15N3O2S	Delayed	Delayed
Mevastatin	C23H34O5	Non effect	Delayed
MK 801 hydrogen maleate	C20H19NO4	Slightly delayed	Delayed
Nabumetone	C15H16O2	Non effect	Severe delayed
Naftopidil dihydrochloride	C24H30Cl2N2O3	Slightly delayed	Delayed
Nandrolone	C18H26O2	Delayed	Delayed
Naproxen sodium salt	C14H13NaO3	Delayed	Delayed
Niclosamide	C13H8Cl2N2O4	Delayed	Delayed
Nifekalant	C19H27N5O5	Delayed	Delayed
Niflumic acid	C13H9F3N2O2	Delayed	Delayed
Nimesulide	C13H12N2O5S	Non effect	Delayed
Nisoldipine	C20H24N2O6	Delayed	Toxic lethal
Nitazoxanide	C12H9N3O5S	Severe delayed	Severe delayed
Norethindrone	C20H26O2	Non effect	Delayed
Norgestimate	C23H31NO3	Slightly delayed	Delayed
Oxfendazol	C15H13N3O3S	Slightly delayed	Delayed
Oxibendazol	C12H15N3O3	Severe delayed	Severe delayed
Oxymetholone	C21H32O3	Slightly delayed	Delayed
Parbendazole	C13H17N3O2	Severe delayed	Severe delayed
Parthenolide	C15H20O3	Non effect	Delayed
Penciclovir	C10H15N5O3	Non effect	Delayed
Pentobarbital	C11H18N2O3	Non effect	Delayed
Phenazopyridine hydrochloride	C11H12ClN5	Delayed	Toxic lethal
Phenothiazine	C12H9NS	Non effect	Delayed
Phenoxybenzamine hydrochloride	C18H23Cl2NO	Non effect	Delayed
Pizotifen malate	C23H27NO5S	Delayed	Severe delayed
Pramoxine hydrochloride	C17H28ClNO3	Slightly delayed	Delayed
Prilocaine hydrochloride	C13H21ClN2O	Non effect	Delayed
Primidone	C12H14N2O2	Slightly delayed	Delayed
Racecadotril	C21H23NO4S	Slightly delayed	Delayed
Riluzole hydrochloride	C8H6ClF3N2OS	Non effect	Delayed
Ritonavir	C37H48N6O5S2	Non effect	Severe delayed
S(-)Eticlopride hydrochloride	C17H26Cl2N2O3	Delayed	Delayed
Salmeterol	C25H37NO4	Non effect	Delayed
Streptomycin sulfate	C42H84N14O36S3	Non effect	Delayed
Sulconazole nitrate	C18H16Cl3N3O3S	Delayed	Delayed
Tegafur	C8H9FN2O3	Delayed	Delayed
Telmisartan	C33H30N4O2	Severe delayed	Toxic lethal
Tenatoprazole	C16H18N4O3S	Non effect	Delayed
Terbinafine	C21H25N	Non effect	Delayed
Thimerosal	C9H9HgNaO2S	Non effect	Delayed
Thiorphan	C12H15NO3S	Delayed	Delayed
Tolcapone	C14H11NO5	Severe delayed	Severe delayed
Topotecan	C23H23N3O5	Delayed	Delayed
Tracazolate hydrochloride	C16H25ClN4O2	Severe delayed	Delayed
Tribenoside	C29H34O6	Delayed	Delayed
Triclabendazole	C14H9Cl3N2OS	Delayed	Delayed
Triclosan	C12H7Cl3O2	Delayed	Severe delayed

Trioxsalen	C14H12O3	Delayed	Delayed
Troglitazone	C24H27NO5S	Severe delayed	Toxic lethal
Valproic acid	C8H16O2	Non effect	Delayed
Voriconazole	C16H14F3N5O	Non effect	Delayed
Zardaverine	C12H10F2N2O3	Slightly delayed	Delayed
Zuclopenthixol dihydrochloride	C22H27Cl3N2OS	Delayed	Delayed

713

714 **Table S2. A list of the drugs that interfere with epiboly progression in zebrafish.**

715 Related to Figure 1.

716 A list of positive "hit" drugs that interfered with epiboly progression. Gastrulation

717 defects or status of each of the zebrafish embryos that were treated with either 10μM

718 or 50μM concentrations, are indicated.

719

720

Table S3. Effects of pharmacological inhibition of HTR2C on metastatic dissemination of MDA-MB-231 cells in zebrafish xenografted models

		Experiment _#1	Experiment _#2	Experiment _#3	Average of Experiments
Drug: Vehicle Cell: MDA-MB-231	Non-dissemination	0% n1=0/17	0% n2=0/12	6.66% n3=1/15	2.22±3.84%
	Head	58.82% n1=10/17	91.66% n2=11/12	6.66% n3=1/15	72.38±17.15%
	Trunk	52.94% n1=9/17	8.33% n2=1/12	20% n3=2/15	27.09±23.13%
	End-tail	100% n1=17/17	100% n2=12/12	86.66% n3=13/15	95.55±7.69%
Drug: Pizotifen Cell: MDA-MB-231	Non-dissemination	55% n1=11/20	31.57% n2=6/19	45.45 % n3=10/22	44.01±11.77%
	Head	5% n1=1/20	31.57% n2=6/19	18.18% n3=4/22	18.25±13.28%
	Trunk	5% n1=1/20	10.52% n2=2/19	4.45% n3=1/22	6.69±3.32%
	End-tail	45% n1=9/20	57.89% n2=11/19	50% n3=11/22	50.96±6.50%

Related to Figure 2D.

The numbers and frequencies of the fish showing the dissemination patterns in vehicle or Pizotifen-treated group, were indicated. The fish showed both patterns of dissemination were redundantly counted in this analysis.

730 **Table S4. Effects of pharmacological inhibition of HTR2C on metastatic**

731 **dissemination of Mia-PaCa2 cells in zebrafish xenografted models**

732

		Experiment _#1	Experiment _#2	Average of Experiments
Drug: Vehicle Cell: MIA-PaCa2	Non-dissemination	17.64% n1=3/17	16.66% n2=2/12	17.15+0.69%
	Head	82.35% n1=14/17	66.66% n2=8/12	74.50+11.09%
	Trunk	29.41% n1=5/17	8.33% n2=1/12	18.87+14.90%
	End-tail	70.58% n1=12/17	83.33% n2=10/17	76.96%+9.01
Drug: Pizotifen Cell: MIA-PaCa2	Non-dissemination	40% n1=4/10	52.63% n2=10/19	46.31+8.93%
	Head	20% n1=2/10	10.52% n2=2/19	15.26+6.69%
	Trunk	10% n1=1/10	5.26% n2=1/19	7.63+3.34%
	End-tail	40% n1=4/10	42.05% n2=8/19	41.4+1.48%

733

734 Related to Figure S3.

735 The numbers and frequencies of the fish showing the dissemination patterns in vehicle

736 or Pizotifen-treated group, were indicated. The fish showed both patterns of

737 dissemination were redundantly counted in this analysis.

738 **Table S5. Effects of genetic inhibition of HTR2C on metastatic dissemination of**

739 **MDA-MB-231 cells in zebrafish xenografted models**

740

		Experiment _#1	Experiment _#2	Average of Experiments
shLacZ	Non-dissemination	0% n1=0/10	0% n2=0/10	0%
	Head	60% n1=6/10	100% n2=10/10	80 ±28.28%
	Trunk	30% n1=3/10	10% n2=1/10	20±14.14%
	End-tail	80% n1=8/10	100% n2=10/10	90%±14.14
shHTR2C	Non-dissemination	80% n1=12/15	76.84% n2=14/19	76.84±4.46 %
	Head	6.66% n1=1/15	15.78% n2=3/19	11.22±6.45%
	Trunk	6.66% n1=1/15	5.26% n2=1/19	5.96±0.99%
	End-tail	20% n1=3/15	26.31% n2=5/19	23.15±4.46%

741

742 Related to Figure 2E.

743 The numbers and frequencies of the fish showing the dissemination patterns in the

744 zebrafish that were inoculated with either shLacZ or shHTR2C MDA-MB-231 cells,

745 were indicated. The fish showed both patterns of dissemination were redundantly

746 counted in this analysis.

Table S6. Effects of HTR2C overexpression on metastatic dissemination of MCF7 cells in zebrafish xenografted models

		Experiment _#1	Experiment _#2	Average of Experiments
VC	Non-dissemination	46.15% n1=6/13	40% n2=4/10	43.07±4.35%
	Head	46.15% n1=6/13	20% n2=2/10	33.07±18.49%
	Trunk	0% n1=0/13	0% n2=0/10	0%
	End-tail	53.84% n1=7/13	60% n2=6/10	56.92±4.35
HTR2C	Non-dissemination	0% n1=0/14	0% n2=0/15	0%
	Head	100% n1=14/14	93.33% n2=14/15	96.66±4.71%
	Trunk	64.28% n1=9/14	73.33% n2=11/15	68.80±6.39%
	End-tail	85.71% n1=12/14	93.33% n2=14/15	89.52±5.38%

Related to Figure 4E.

The numbers and frequencies of the fish showing the dissemination patterns in the zebrafish that were inoculated with MCF7 cells expressing either VC or HTR2C, were indicated. The fish showed both patterns of dissemination were redundantly counted in this analysis.

References for Table S1.

1. Kondo M (2007) Bone morphogenetic proteins in the early development of zebrafish. *FEBS J* 274(12):2960-2967.
2. Katsuno Y, *et al.* (2008) Bone morphogenetic protein signaling enhances invasion and bone metastasis of breast cancer cells through Smad pathway. *Oncogene* 27(49):6322-6333.
3. Tada M & Smith JC (2000) Xwnt11 is a target of Xenopus Brachyury: regulation of gastrulation movements via Dishevelled, but not through the canonical Wnt pathway. *Development* 127:2227-2238.
4. Vincan E & Barker N (2008) The upstream components of the Wnt signalling pathway in the dynamic EMT and MET associated with colorectal cancer progression. *Clin Exp Metastasis* 25(6):657-663.
5. Yang X, Dormann D, Munsterberg AE, & Weijer CJ (2002) Cell movement patterns during gastrulation in the chick are controlled by positive and negative chemotaxis mediated by FGF4 and FGF8. *Dev Cell* 3(3):425-437.
6. Nomura S, *et al.* (2008) FGF10/FGFR2 signal induces cell migration and invasion in pancreatic cancer. *Br J Cancer* 99(2):305-313.

7. Song S, *et al.* (2013) Pou5f1-dependent EGF expression controls E-cadherin endocytosis, cell adhesion, and zebrafish epiboly movements. *Dev Cell* 24(5):486-501.
8. Lu Z, Jiang G, Blume-Jensen P, & Hunter T (2001) Epidermal growth factor-induced tumor cell invasion and metastasis initiated by dephosphorylation and downregulation of focal adhesion kinase. *Mol Cell Biol* 21(12):4016-4031.
9. Damm EW & Winklbauer R (2011) PDGF-A controls mesoderm cell orientation and radial intercalation during Xenopus gastrulation. *Development* 138(3):565-575.
10. Jechlinger M, *et al.* (2006) Autocrine PDGFR signaling promotes mammary cancer metastasis. *J Clin Invest* 116(6):1561-1570.
11. Mizoguchi T, Verkade H, Heath JK, Kuroiwa A, & Kikuchi Y (2008) Sdf1/Cxcr4 signaling controls the dorsal migration of endodermal cells during zebrafish gastrulation. *Development* 135(15):2521-2529.
12. Shen HB, Gu ZQ, Jian K, & Qi J (2013) CXCR4-mediated Stat3 activation is essential for CXCL12-induced cell invasion in bladder cancer. *Tumour Biol* 34(3):1839-1845.
13. Montero J-A, Kilian B, Chan J, Bayliss PE, & Heisenberg C-P (2003) Phosphoinositide 3-Kinase Is Required for Process Outgrowth and Cell Polarization of Gastrulating Mesendodermal Cells. *Current Biology* 13(15):1279-1289.
14. Wander SA, *et al.* (2013) PI3K/mTOR inhibition can impair tumor invasion and metastasis in vivo despite a lack of antiproliferative action in vitro: implications for targeted therapy. *Breast Cancer Res Treat* 138(2):369-381.
15. Tsai WB, Zhang X, Sharma D, Wu W, & Kinsey WH (2005) Role of Yes kinase during early zebrafish development. *Dev Biol* 277(1):129-141.
16. Barraclough J, Hodgkinson C, Hogg A, Dive C, & Welman A (2007) Increases in c-Yes Expression Level and Activity Promote Motility But Not Proliferation of Human Colorectal Carcinoma Cells. *Neoplasia* 9(9):745-IN732.
17. Sharma D, Holets L, Zhang X, & Kinsey WH (2005) Role of Fyn kinase in signaling associated with epiboly during zebrafish development. *Dev Biol* 285(2):462-476.
18. Yadav V & Denning MF (2011) Fyn is induced by Ras/PI3K/Akt signaling and is required for enhanced invasion/migration. *Mol Carcinog* 50(5):346-352.
19. Krens SF, *et al.* (2008) Distinct functions for ERK1 and ERK2 in cell migration processes during zebrafish gastrulation. *Dev Biol* 319(2):370-383.
20. Radtke S, Milanovic M, & Rossé C (2013) ERK2 but not ERK1 mediates HGF-induced motility in non-small cell lung carcinoma cell lines. *J Cell Sci.* 126(Pt11):2381-2391.
21. Jopling C, van Geemen D, & den Hertog J (2007) Shp2 knockdown and Noonan/LEOPARD mutant Shp2-induced gastrulation defects. *PLoS Genet* 3(12):e225.
22. Wang FM, *et al.* (2005) SHP-2 promoting migration and metastasis of MCF-7 with loss of E-cadherin, dephosphorylation of FAK and secretion of MMP-9 induced by IL-1beta in vivo and in vitro. *Breast Cancer Res Treat* 89(1):5-14.
23. Ip YT & Gridley T (2002) Cell movements during gastrulation: snail dependent and independent pathways. *Curr Opin Genet Dev* 12(4):423-429.
24. Batlle E, Sancho E, Francí C, Domínguez D, & Monfar M (2000) The transcription factor snail is a repressor of E-cadherin gene expression in epithelial tumour cells. *Nat Cell Biol* 2(2):84-89.
25. Shi J, Severson C, Yang J, Wedlich D, & Klymkowsky MW (2011) Snail2 controls mesodermal BMP/Wnt induction of neural crest. *Development* 138(15):3135-3145.

26. Castanon I & Baylies MK (2002) A Twist in fate: evolutionary comparison of Twist structure and function. *Gene* 287(1-2):11-22.
27. Yang J, *et al.* (2004) Twist, a master regulator of morphogenesis, plays an essential role in tumor metastasis. *Cell* 117(7):927-939.
28. Fernando RI, *et al.* (2010) The T-box transcription factor Brachyury promotes epithelial-mesenchymal transition in human tumor cells. *J Clin Invest* 120(2):533-544.
29. Vannier C, Mock K, Brabletz T, & Driever W (2013) Zeb1 regulates E-cadherin and Epcam (epithelial cell adhesion molecule) expression to control cell behavior in early zebrafish development. *J Biol Chem* 288(26):18643-18659.
30. Spaderna S, *et al.* (2008) The transcriptional repressor ZEB1 promotes metastasis and loss of cell polarity in cancer. *Cancer Res* 68(2):537-544.
31. Sander V, Reversade B, & De Robertis EM (2007) The opposing homeobox genes Goosecoid and Vent1/2 self-regulate Xenopus patterning. *EMBO J* 26(12):2955-2965.
32. Hartwell KA, *et al.* (2006) The Spemann organizer gene, Goosecoid, promotes tumor metastasis. *Proc Natl Acad Sci U S A* 103(50):18969-18974.
33. Wilm B, James RG, Schultheiss TM, & Hogan BL (2004) The forkhead genes, Foxc1 and Foxc2, regulate paraxial versus intermediate mesoderm cell fate. *Dev Biol* 271(1):176-189.
34. Mani SA, *et al.* (2007) Mesenchyme Forkhead 1 (FOXC2) plays a key role in metastasis and is associated with aggressive basal-like breast cancers. *Proc Natl Acad Sci U S A* 104(24):10069-10074.
35. Miyagi C, *et al.* (2004) STAT3 noncell-autonomously controls planar cell polarity during zebrafish convergence and extension. *J Cell Biol* 166(7):975-981.
36. Abdulghani J, *et al.* (2008) Stat3 promotes metastatic progression of prostate cancer. *Am J Pathol* 172(6):1717-1728.
37. Lachnit M, Kur E, & Driever W (2008) Alterations of the cytoskeleton in all three embryonic lineages contribute to the epiboly defect of Pou5f1/Oct4 deficient MZspg zebrafish embryos. *Dev Biol* 315(1):1-17.
38. Dai X, *et al.* (2013) OCT4 regulates epithelial-mesenchymal transition and its knockdown inhibits colorectal cancer cell migration and invasion. *Oncol Rep* 29(1):155-160.
39. O'Carroll D, *et al.* (2001) The polycomb-group gene Ezh2 is required for early mouse development. *Mol Cell Biol* 21(13):4330-4336.
40. Ren G, *et al.* (2012) Polycomb protein EZH2 regulates tumor invasion via the transcriptional repression of the metastasis suppressor RKIP in breast and prostate cancer. *Cancer Res* 72(12):3091-3104.
41. Lin F, *et al.* (2005) Essential roles of G{alpha}12/13 signaling in distinct cell behaviors driving zebrafish convergence and extension gastrulation movements. *J Cell Biol* 169(5):777-787.
42. Chen MW, *et al.* (2010) H3K9 histone methyltransferase G9a promotes lung cancer invasion and metastasis by silencing the cell adhesion molecule Ep-CAM. *Cancer Res* 70(20):7830-7840.
43. van der Lugt NM, *et al.* (1994) Posterior transformation, neurological abnormalities, and severe hematopoietic defects in mice with a targeted deletion of the bmi-1 proto-oncogene. *Genes Dev* 8(7):757-769.
44. Guo BH, *et al.* (2011) Bmi-1 promotes invasion and metastasis, and its elevated expression is correlated with an advanced stage of breast cancer. *Mol Cancer* 10(1):10.
45. Zhu S, Liu L, Korzh V, Gong Z, & Low BC (2006) RhoA acts downstream of Wnt5 and Wnt11 to regulate convergence and extension movements by

involving effectors Rho kinase and Diaphanous: use of zebrafish as an in vivo model for GTPase signaling. *Cell Signal* 18(3):359-372.

46. Yoshioka K, Nakamori S, & Itoh K (1999) Overexpression of small GTP-binding protein RhoA promotes invasion of tumor cells. *Cancer Res* 59(8):2004-2010.

47. Choi SC & Han JK (2002) Xenopus Cdc42 regulates convergent extension movements during gastrulation through Wnt/Ca2+ signaling pathway. *Dev Biol* 244(2):342-357.

48. Reymond N, *et al.* (2012) Cdc42 promotes transendothelial migration of cancer cells through beta1 integrin. *J Cell Biol* 199(4):653-668.

49. Habas R, Dawid IB, & He X (2003) Coactivation of Rac and Rho by Wnt/Frizzled signaling is required for vertebrate gastrulation. . *Genes Dev* 17(2):295-309.

50. Vega FM & Ridley AJ (2008) Rho GTPases in cancer cell biology. *FEBS Lett* 582(14):2093-2101.

51. Marlow F, Topczewski J, Sepich D, & Solnica-Krezel L (2002) Zebrafish Rho kinase 2 acts downstream of Wnt11 to mediate cell polarity and effective convergence and extension movements. *Curr Biol* 12(11):876-884.

52. Itoh K, *et al.* (1999) An essential part for Rho-associated kinase in the transcellular invasion of tumor cells. *Nat Med* 5(2):221-225.

53. Kusakabe M & Nishida E (2004) The polarity-inducing kinase Par-1 controls Xenopus gastrulation in cooperation with 14-3-3 and aPKC. *EMBO J* 23(21):4190-4201.

54. Shi X, Gangadharan B, Brass LF, Ruf W, & Mueller BM (2004) Protease-activated receptors (PAR1 and PAR2) contribute to tumor cell motility and metastasis. *Mol Cancer Res* 2(7):395-402.

55. Gunaratne A, Thai BL, & Di Guglielmo GM (2013) Atypical protein kinase C phosphorylates Par6 and facilitates transforming growth factor beta-induced epithelial-to-mesenchymal transition. *Mol Cell Biol* 33(5):874-886.

56. Seifert K, Ibrahim H, Stodtmeister T, Winklbauer R, & Niessen CM (2009) An adhesion-independent, aPKC-dependent function for cadherins in morphogenetic movements. *J Cell Sci* 122(Pt 14):2514-2523.

57. Yamazaki K, *et al.* (2009) Adenylate cyclase-associated protein 1 overexpressed in pancreatic cancers is involved in cancer cell motility. *Lab Invest* 89(4):425-432.

58. Link V, *et al.* (2006) Identification of regulators of germ layer morphogenesis using proteomics in zebrafish. *J Cell Sci* 119(Pt 10):2073-2083.

59. Khanna C, *et al.* (2004) The membrane-cytoskeleton linker ezrin is necessary for osteosarcoma metastasis. *Nat Med* 10(2):182-186.

60. Slanchev K, *et al.* (2009) The epithelial cell adhesion molecule EpCAM is required for epithelial morphogenesis and integrity during zebrafish epiboly and skin development. *PLoS Genet* 5(7):e1000563.

61. Ni J, *et al.* (2012) Role of the EpCAM (CD326) in prostate cancer metastasis and progression. *Cancer Metastasis Rev* 31(3-4):779-791.

62. Skalski M, Alfandari D, & Darribere T (1998) A key function for alphav containing integrins in mesodermal cell migration during Pleurodeles waltl gastrulation. *Dev Biol* 195(2):158-173.

63. Felding-Habermann B (2003) Integrin adhesion receptors in tumor metastasis. *Clin Exp Metastasis* 20(3):203-213.

64. Marsden M & DeSimone DW (2003) Integrin-ECM Interactions Regulate Cadherin-Dependent Cell Adhesion and Are Required for Convergent Extension in Xenopus. *Current Biology* 13(14):1182-1191.

65. Malik G, *et al.* (2010) Plasma fibronectin promotes lung metastasis by contributions to fibrin clots and tumor cell invasion. *Cancer Res* 70(11):4327-4334.
66. Bakkers J, *et al.* (2004) Has2 is required upstream of Rac1 to govern dorsal migration of lateral cells during zebrafish gastrulation. *Development* 131(3):525-537.
67. Kim HR, *et al.* (2004) Hyaluronan facilitates invasion of colon carcinoma cells in vitro via interaction with CD44. *Cancer Res* 64(13):4569-4576.
68. Coyle RC, Latimer A, & Jessen JR (2008) Membrane-type 1 matrix metalloproteinase regulates cell migration during zebrafish gastrulation: evidence for an interaction with non-canonical Wnt signaling. *Exp Cell Res* 314(10):2150-2162.
69. Perentes JY, *et al.* (2011) Cancer cell-associated MT1-MMP promotes blood vessel invasion and distant metastasis in triple-negative mammary tumors. *Cancer Res* 71(13):4527-4538.
70. Cha YI, *et al.* (2006) Cyclooxygenase-1-derived PGE2 promotes cell motility via the G-protein-coupled EP4 receptor during vertebrate gastrulation. *Genes Dev* 20(1):77-86.
71. Kundu N & Fulton AM (2002) Selective cyclooxygenase (COX)-1 or COX-2 inhibitors control metastatic disease in a murine model of breast cancer. *Cancer Res* 62(8):2343-2346.
72. Speirs CK, *et al.* (2010) Prostaglandin Gbetagamma signaling stimulates gastrulation movements by limiting cell adhesion through Snai1a stabilization. *Development* 137(8):1327-1337.
73. Wang D & Dubois RN (2006) Prostaglandins and cancer. *Gut* 55(1):115-122.
74. Yamashita S, *et al.* (2004) Zinc transporter LIVI controls epithelial-mesenchymal transition in zebrafish gastrula organizer. *Nature* 429(6989):298-302.
75. Lue HW, *et al.* (2011) LIV-1 promotes prostate cancer epithelial-to-mesenchymal transition and metastasis through HB-EGF shedding and EGFR-mediated ERK signaling. *PLoS One* 6(11):e27720.
76. Yagi H, *et al.* (2011) A synthetic biology approach reveals a CXCR4-G13-Rho signaling axis driving transendothelial migration of metastatic breast cancer cells. *Sci Signal* 4(191):ra60.
77. Webster DM, *et al.* (2009) O-GlcNAc modifications regulate cell survival and epiboly during zebrafish development. *BMC Dev Biol* 9:28.
78. Lynch TP, *et al.* (2012) Critical role of O-Linked beta-N-acetylglucosamine transferase in prostate cancer invasion, angiogenesis, and metastasis. *J Biol Chem* 287(14):11070-11081.
79. Latinkic BV (2003) Xenopus Cyr61 regulates gastrulation movements and modulates Wnt signalling. *Development* 130(11):2429-2441.
80. Lin J, *et al.* (2012) A novel anti-Cyr61 antibody inhibits breast cancer growth and metastasis in vivo. *Cancer Immunol Immunother* 61(5):677-687.
81. Liu W, *et al.* (2011) TRPM7 regulates gastrulation during vertebrate embryogenesis. *Dev Biol* 350(2):348-357.
82. Middelbeek J, *et al.* (2012) TRPM7 is required for breast tumor cell metastasis. *Cancer Res* 72(16):4250-4261.
83. Holloway BA, *et al.* (2009) A novel role for MAPKAPK2 in morphogenesis during zebrafish development. *PLoS Genet* 5(3):e1000413.
84. Kumar B, *et al.* (2010) p38 mitogen-activated protein kinase-driven MAPKAPK2 regulates invasion of bladder cancer by modulation of MMP-2 and MMP-9 activity. *Cancer Res* 70(2):832-841.

85. Machingo QJ, Fritz A, & Shur BD (2006) A beta1,4-galactosyltransferase is required for convergent extension movements in zebrafish. *Dev Biol* 297(2):471-482.
86. Zhu X, *et al.* (2005) Elevated beta1,4-galactosyltransferase I in highly metastatic human lung cancer cells. Identification of E1AF as important transcription activator. *J Biol Chem* 280(13):12503-12516.
87. Hong SK, Tanegashima K, & Dawid IB (2011) XIer2 is required for convergent extension movements during Xenopus development. *Int J Dev Biol* 55(10-12):917-921.
88. Neeb A, *et al.* (2012) The immediate early gene Ier2 promotes tumor cell motility and metastasis, and predicts poor survival of colorectal cancer patients. *Oncogene* 31(33):3796-3806.
89. Besser J, Leito JT, van der Meer DL, & Bagowski CP (2007) Tip-1 induces filopodia growth and is important for gastrulation movements during zebrafish development. *Dev Growth Differ* 49(3):205-214.
90. Han M, Wang H, Zhang HT, & Han Z (2012) The PDZ protein TIP-1 facilitates cell migration and pulmonary metastasis of human invasive breast cancer cells in athymic mice. *Biochem Biophys Res Commun* 422(1):139-145.
91. Faure S, *et al.* (2005) Xenopus p21-activated kinase 5 regulates blastomeres' adhesive properties during convergent extension movements. *Dev Biol* 277(2):472-492.
92. Gong W, *et al.* (2009) P21-activated kinase 5 is overexpressed during colorectal cancer progression and regulates colorectal carcinoma cell adhesion and migration. *Int J Cancer* 125(3):548-555.
93. Iioka H, Ueno N, & Kinoshita N (2004) Essential role of MARCKS in cortical actin dynamics during gastrulation movements. *J Cell Biol* 164(2):169-174.
94. Rombouts K, *et al.* (2013) Myristoylated Alanine-Rich protein Kinase C Substrate (MARCKS) expression modulates the metastatic phenotype in human and murine colon carcinoma in vitro and in vivo. *Cancer Lett* 333(2):244-252.
95. Medici D, Hay ED, & B.R. O (2008) Snail and Slug Promote Epithelial-Mesenchymal Transition through -Catenin–T-Cell Factor-4-dependent Expression of Transforming Growth Factor-3. Molecular Biology of the Cell 19(11):4875–4887.

Source data and legend for source data

Figure 2a_HRT2C_source data

Western blot analysis of HRT2C protein levels in non-metastatic human cancer cell line, MCF7 (breast) and highly metastatic human cancer cell lines, MDA-MB-231 (breast), MDA-MB-435 (melanoma), MIA-PaCa2 (pancreas), SW620 (colon) and PC3 (prostate).

Figure 2a_GAPDH_source data

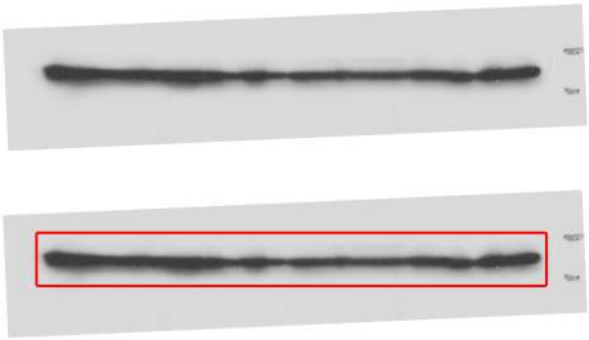

Western blot analysis of GAPDH protein levels in non-metastatic human cancer cell line, MCF7 (breast) and highly metastatic human cancer cell lines, MDA-MB-231 (breast), MDA-MB-435 (melanoma), MIA-PaCa2 (pancreas), SW620 (colon) and PC3 (prostate).

Figure 4C_E-cadherin in MCF7_ source data

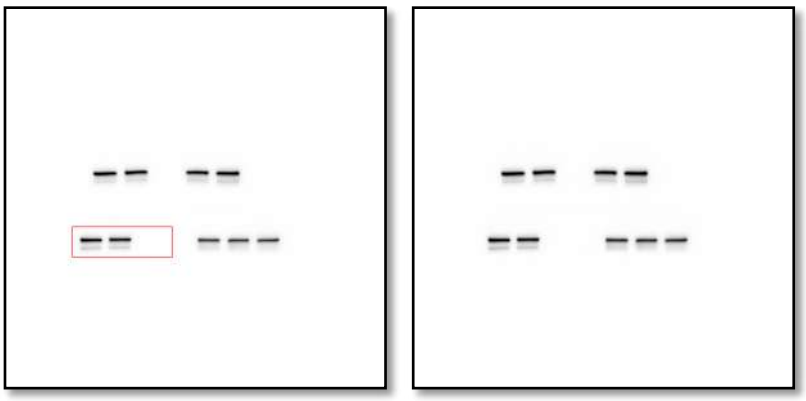

Western blot analysis of E-cadherin protein levels in MCF7 cells expressing either the control vector or HTR2C.

Figure 4C_EpCAM in MCF7_ source data

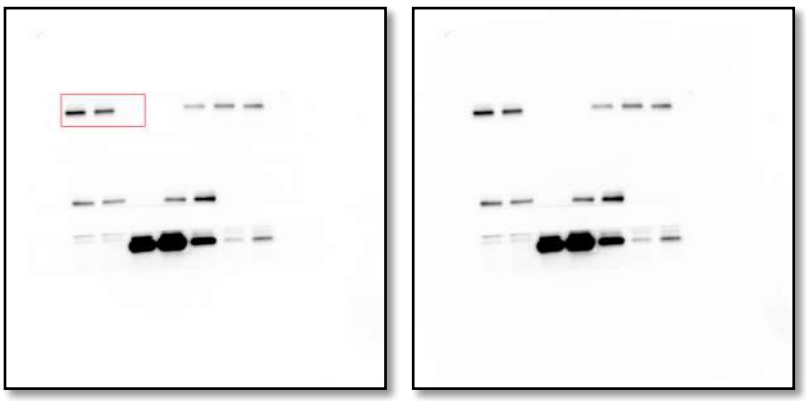

Western blot analysis of EpCAM protein levels in MCF7 cells expressing either the control vector or HTR2C.

Figure 4C_Vimentin in MCF7_ source data

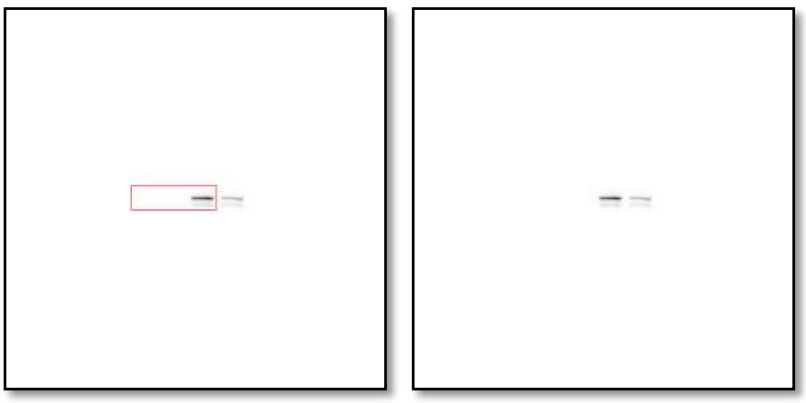

Western blot analysis of Vimentin protein levels in MCF7 cells expressing either the control vector or HTR2C.

Figure 4C_N-cadherin in MCF7_ source data

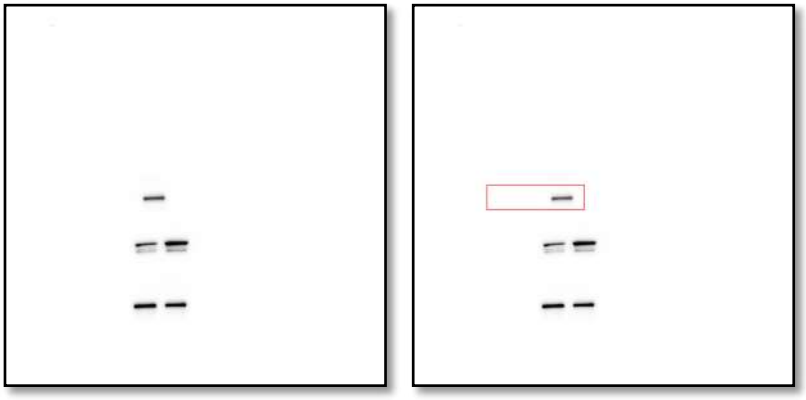

Western blot analysis of N-cadherin protein levels in MCF7 cells expressing either the control vector or HTR2C.

Figure 4C_Zeb1 in MCF7_ source data

Western blot analysis of Zeb1 protein levels in MCF7 cells expressing either the control vector or HTR2C.

Figure 4C_HRT2C in MCF7_ source data

Western blot analysis of HRT2C protein levels in MCF7 cells expressing either the control vector or HTR2C.

Figure 4C_GAPDH in MCF7_source data

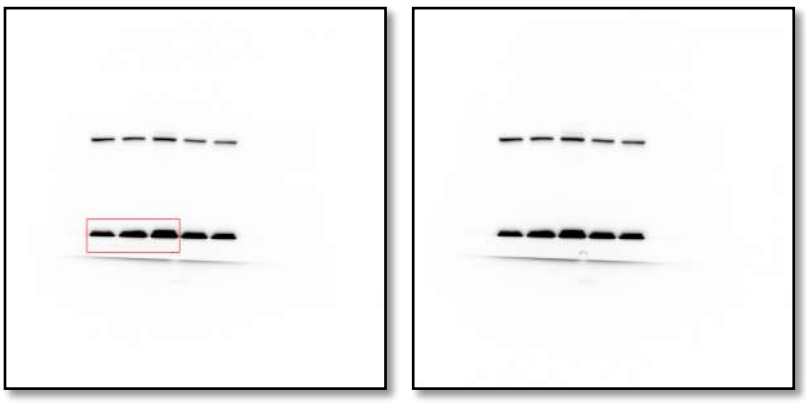

Western blot analysis of GAPDH protein levels in MCF7 cells expressing either the control vector or HTR2C.

Figure 4C_E-cadherin in HaCaT_source data

1074 Western blot analysis of E-cadherin protein levels in HaCaT cells expressing either

1075 the control vector or HTR2C.

1076

1077 **Figure 4C_EpCAM in HaCaT_source data**

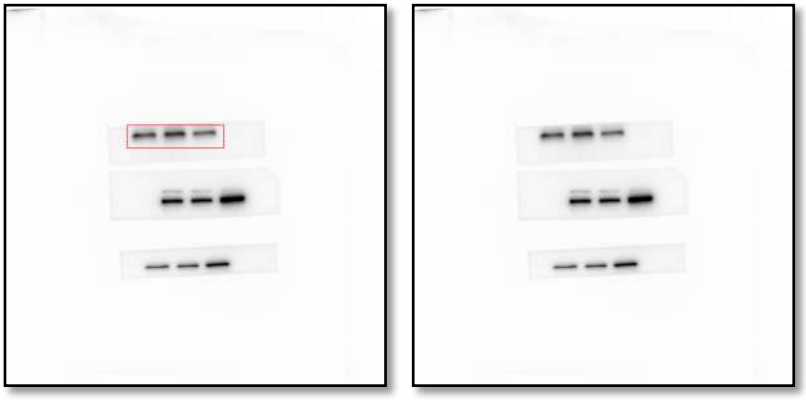

1078

1079 Western blot analysis of EpCAM protein levels in HaCaT cells expressing either the

1080 control vector or HTR2C.

1081

1082 **Figure 4C_Vimentin in HaCaT_source data**

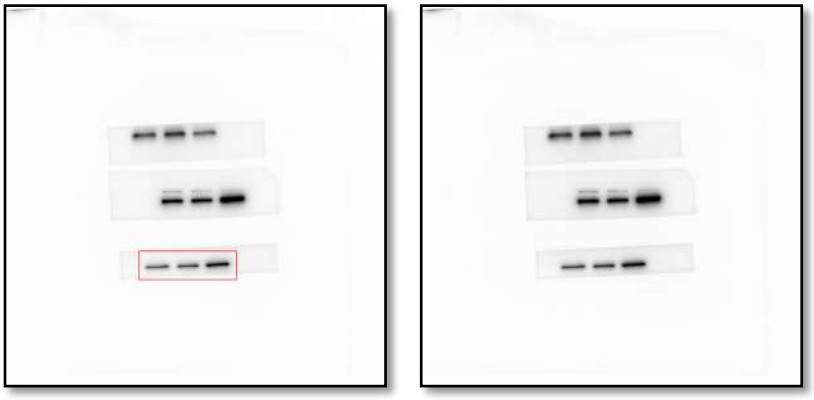

1083

1084 Western blot analysis of Vimentin protein levels in HaCaT cells expressing either the

1085 control vector or HTR2C.

1086

1087 **Figure 4C_N-cadherin in HaCaT_source data**

Western blot analysis of N-cadherin protein levels in HaCaT cells expressing either the control vector or HTR2C.

Figure 4C_Zeb1 in HaCaT source data

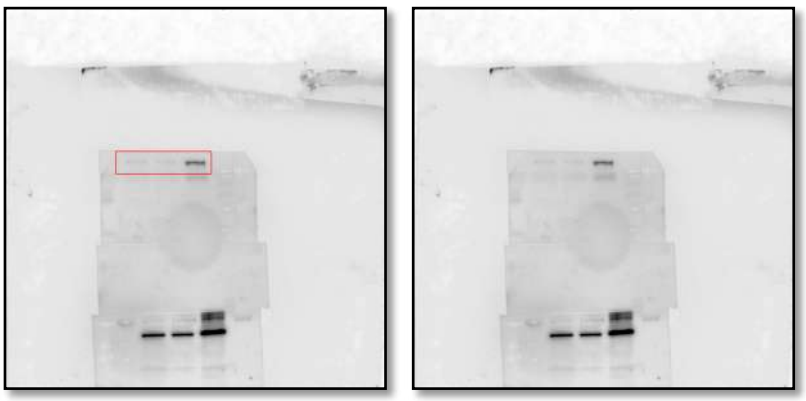

Western blot analysis of zeb1 protein levels in HaCaT cells expressing either the control vector or HTR2C.

Figure 4C_HRT2C in HaCaT_source data

Western blot analysis of HRT2C protein levels in HaCaT cells expressing either the control vector or HTR2C.

Figure 4C_GAPDH in HaCaT_source data

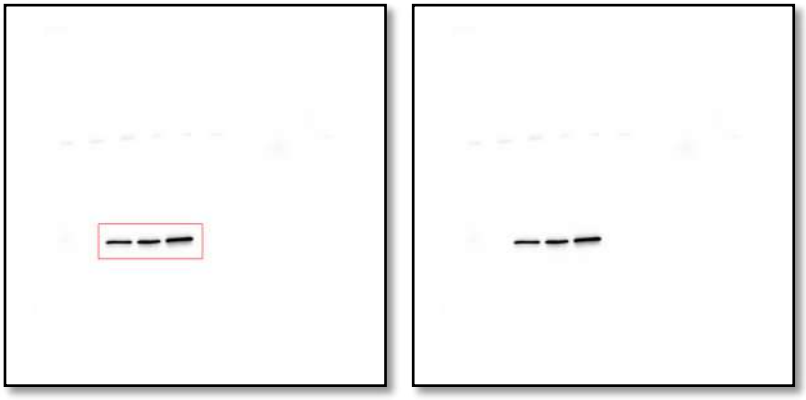

Western blot analysis of GAPDH protein levels in HaCaT cells expressing either the control vector or HTR2C.

Figure 5C_E-cadherin_source data

Western blot analysis of E-cadherin protein levels in whole cell lysate of 4T1 primary tumors from either vehicle or Pizotifen-treated mice.

Figure 5C_Zeb1 _source data

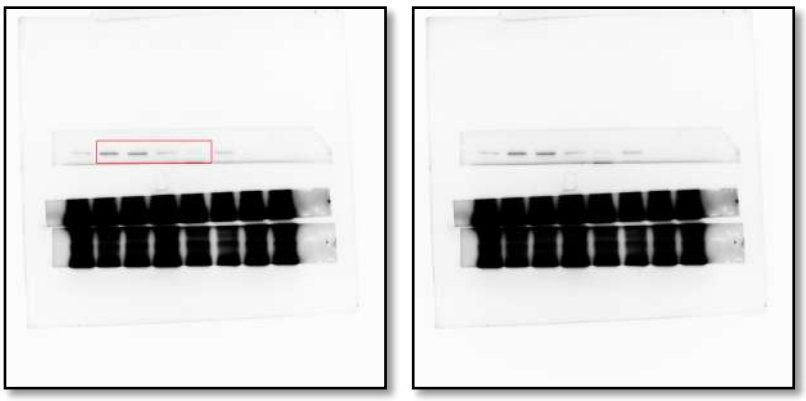

Western blot analysis of Zeb1 protein levels in whole cell lysate of 4T1 primary tumors from either vehicle or Pizotifen-treated mice.

Figure 5C_ Phosphorylation of serine-9 in GSK3β_source data

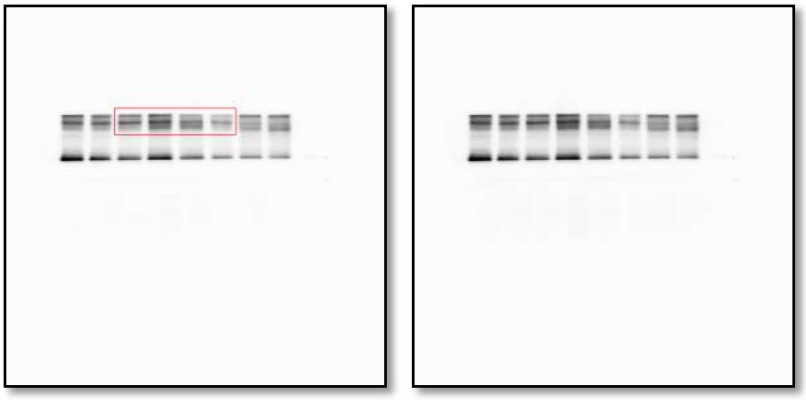

Western blot analysis of the protein levels of phosphorylation of serine-9 in GSK3β in whole cell lysate of 4T1 primary tumors from either vehicle or Pizotifen-treated mice.

Figure 5C_ GSK3β_source data

Western blot analysis of GSK3β protein levels in whole cell lysate of 4T1 primary tumors from either vehicle or Pizotifen-treated mice.

Figure 5C_Luciferase_source data

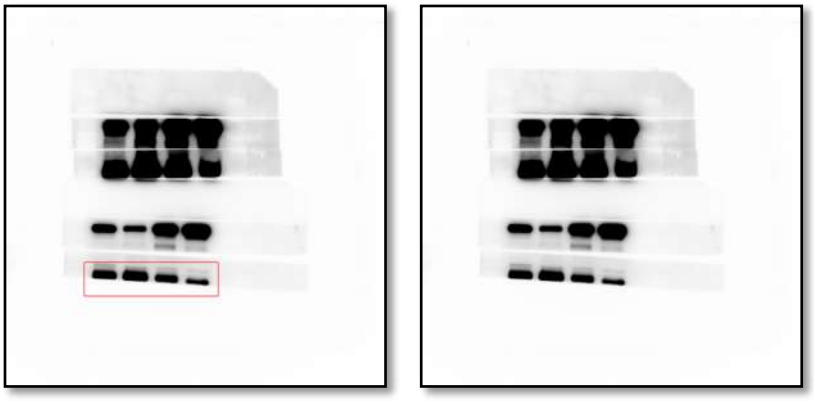

Western blot analysis of Luciferase protein levels in whole cell lysate of 4T1 primary tumors from either vehicle or Pizotifen-treated mice.

Figure 5C_β-catenin in the nucleus_source data

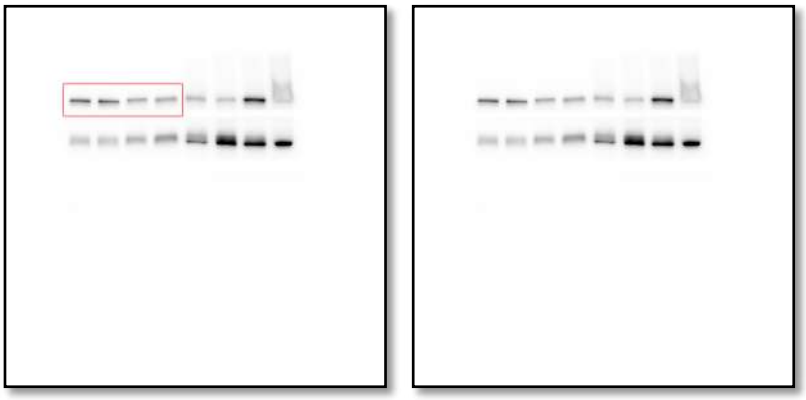

Western blot analysis of β-catenin protein levels in the nucleus of 4T1 primary tumors from either vehicle or Pizotifen-treated mice.

Figure 5C_Histone H3 in the nucleus_source data

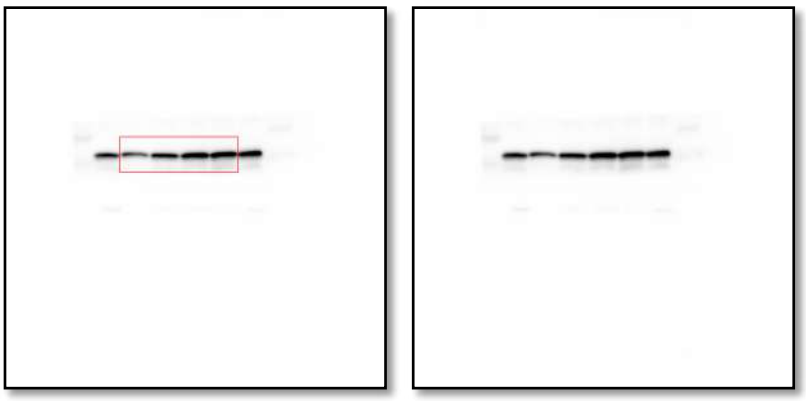

Western blot analysis of Histone H3 protein levels in the nucleus of 4T1 primary tumors from either vehicle or Pizotifen-treated mice.

Figure 5C_β-catenin in the cytoplasm_source data

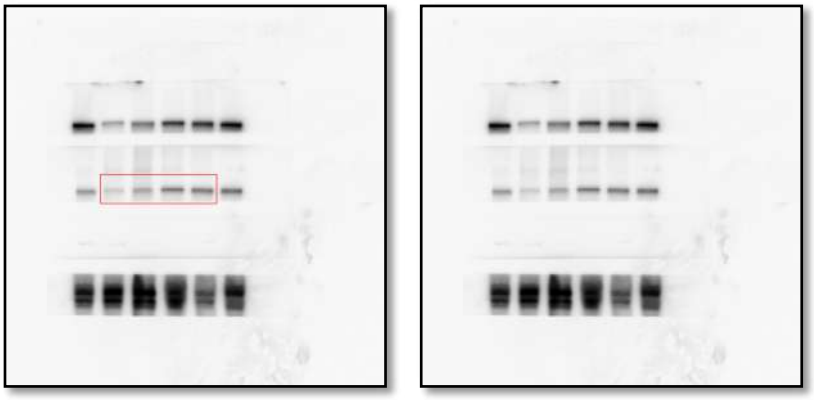

Western blot analysis of β-catenin protein levels in the cytoplasm of 4T1 primary tumors from either vehicle or Pizotifen-treated mice.

Figure 5C_β-tubulin in the cytoplasm_source data

Western blot analysis of β-tubulin protein levels in the cytoplasm of 4T1 primary tumors from either vehicle or Pizotifen-treated mice.

Figure 5D_E-cadherin_source data

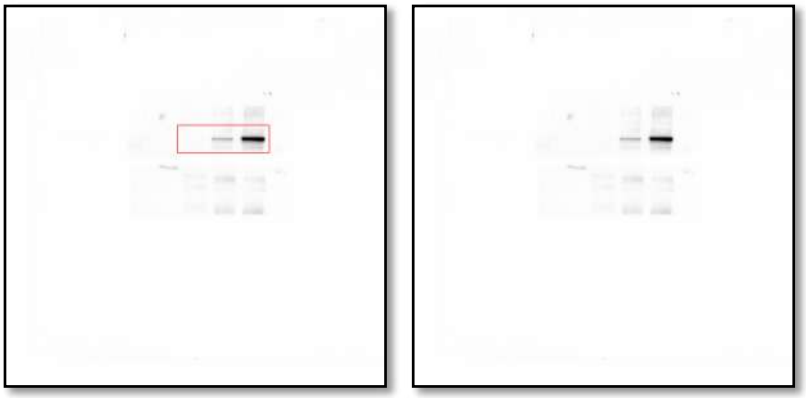

Western blot analysis of E-cadherin protein levels in either vehicle or Pizotifen-treated MDA-MB-231 cells or E-cadherin positive cells in Pizotifen-treated MDA-MB-231 cells.

Figure 5D_EpCAM_source data

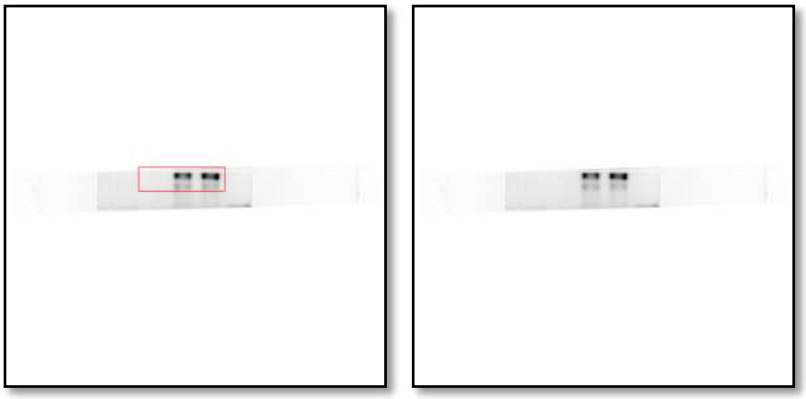

Western blot analysis of EpCAM protein levels in either vehicle or Pizotifen-treated MDA-MB-231 cells or E-cadherin positive cells in Pizotifen-treated MDA-MB-231 cells.

Figure 5D_Keratin18 (KRT18)_source data

Western blot analysis of KRT18 protein levels in either vehicle or Pizotifen-treated MDA-MB-231 cells or E-cadherin positive cells in Pizotifen-treated MDA-MB-231 cells.

Figure 5D_Keratin19 (KRT19)_source data

Western blot analysis of KRT19 protein levels in either vehicle or Pizotifen-treated MDA-MB-231 cells or E-cadherin positive cells in Pizotifen-treated MDA-MB-231 cells.

Figure 5D_Vimentin_source data

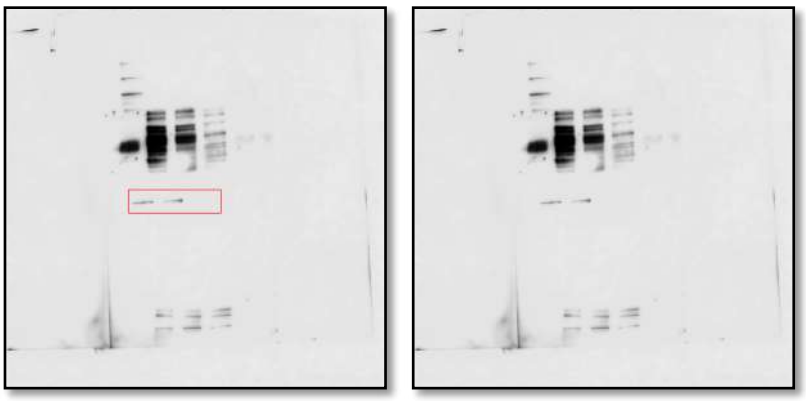

Western blot analysis of Vimentin protein levels in either vehicle or Pizotifen-treated MDA-MB-231 cells or E-cadherin positive cells in Pizotifen-treated MDA-MB-231 cells.

Figure 5D_MMP1_source data

Western blot analysis of MMP1 protein levels in either vehicle or Pizotifen-treated MDA-MB-231 cells or E-cadherin positive cells in Pizotifen-treated MDA-MB-231 cells.

Figure 5D_MMP3_source data

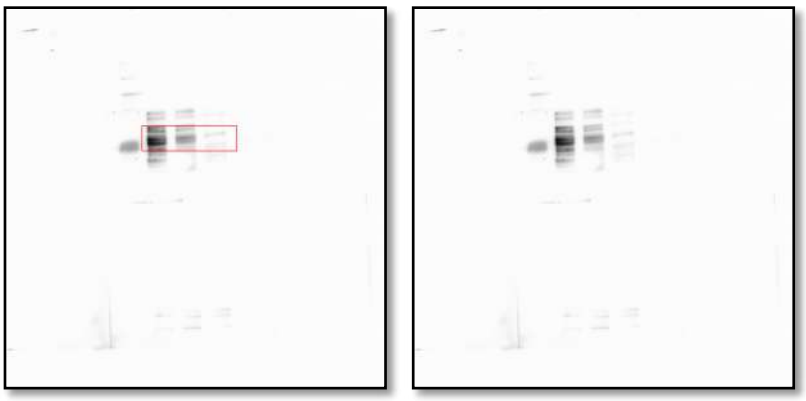

Western blot analysis of MMP3 protein levels in either vehicle or Pizotifen-treated MDA-MB-231 cells or E-cadherin positive cells in Pizotifen-treated MDA-MB-231 cells.

Figure 5D_S100A4_source data

Western blot analysis of S100A4 protein levels in either vehicle or Pizotifen-treated MDA-MB-231 cells or E-cadherin positive cells in Pizotifen-treated MDA-MB-231 cells.

Figure 5D_Zeb1_source data

Western blot analysis of Zeb1 protein levels in either vehicle or Pizotifen-treated MDA-MB-231 cells or E-cadherin positive cells in Pizotifen-treated MDA-MB-231 cells.

Figure 5D_GAPDH_source data

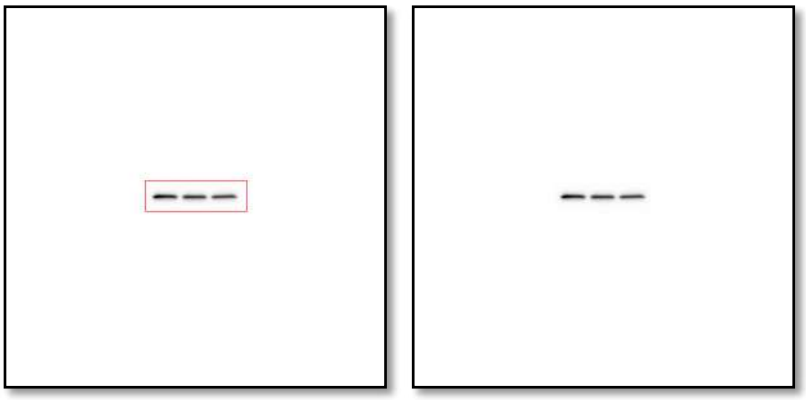

Western blot analysis of GAPDH protein levels in either vehicle or Pizotifen-treated MDA-MB-231 cells or E-cadherin positive cells in Pizotifen-treated MDA-MB-231 cells.

Figure 5F_β-catenin in the nucleus_source data

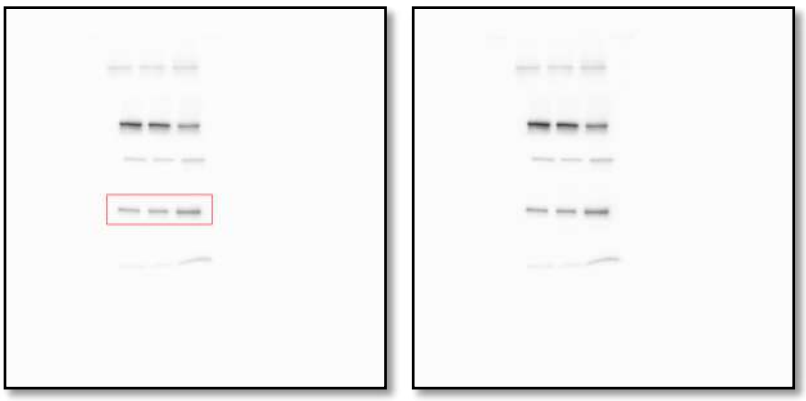

Western blot analysis of β-catenin protein levels in the nuclear of MCF7 cells expressing either the control vector or HTR2C.

Figure 5F_Histone H3 in the nucleus _source data

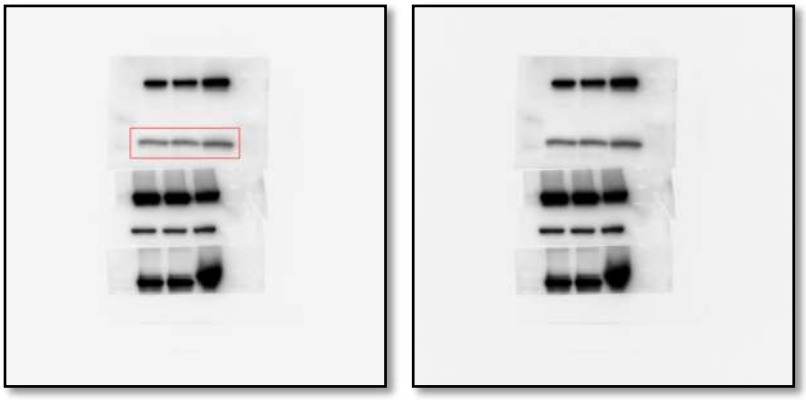

Western blot analysis of Histone H3 protein levels in the nuclear of MCF7 cells expressing either the control vector or HTR2C.

Figure 5F_β-catenin in the cytoplasm_source data

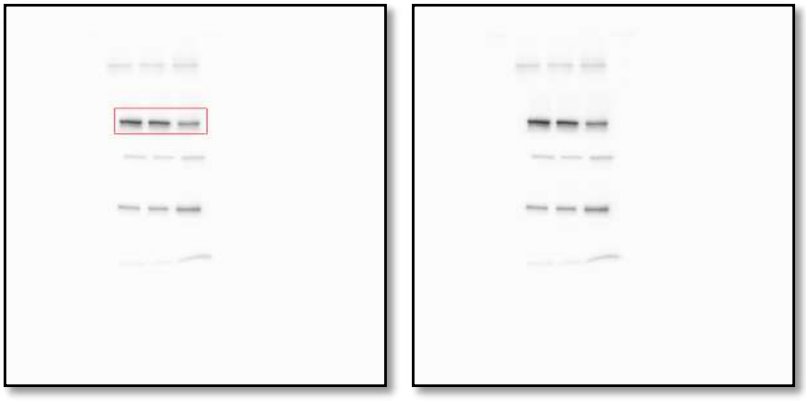

1225 Western blot analysis of β-catenin protein levels in the cytoplasm of MCF7 cells

1226 expressing either the control vector or HTR2C.

1227

1228 **Figure 5F_β-tubulin in the cytoplasm_source data**

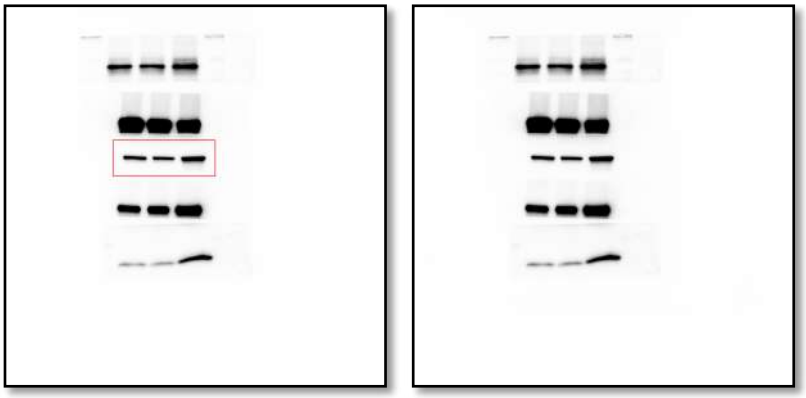

1229

1230 Western blot analysis of β-tubulin protein levels in the cytoplasm of MCF7 cells

1231 expressing either the control vector or HTR2C.

1232

1233 **Figure 5F_Phosphorylation of serine-9 in GSK3β_source data**

1234

1235 Western blot analysis of the protein levels of phosphorylation of serine-9 in GSK3β in

1236 whole cell lysate of MCF7 cells expressing either the control vector or HTR2C.

1237

1238 **Figure 5F_GSK3β_source data**

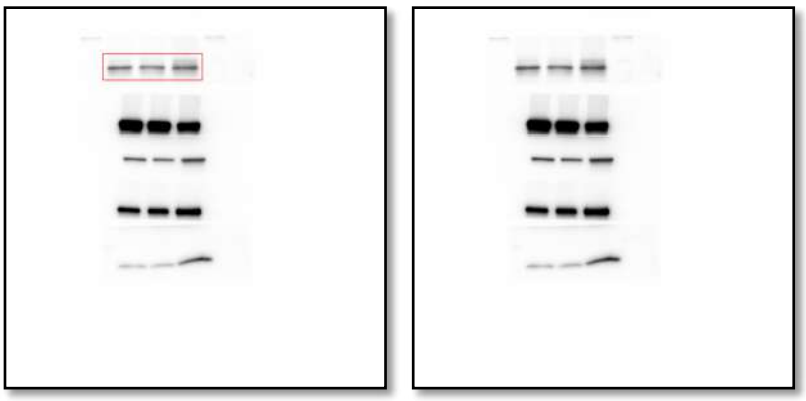

Western blot analysis of GSK3β protein levels in whole cell lysate of MCF7 cells expressing either the control vector or HTR2C.

Figure 5F_GAPDH_source data

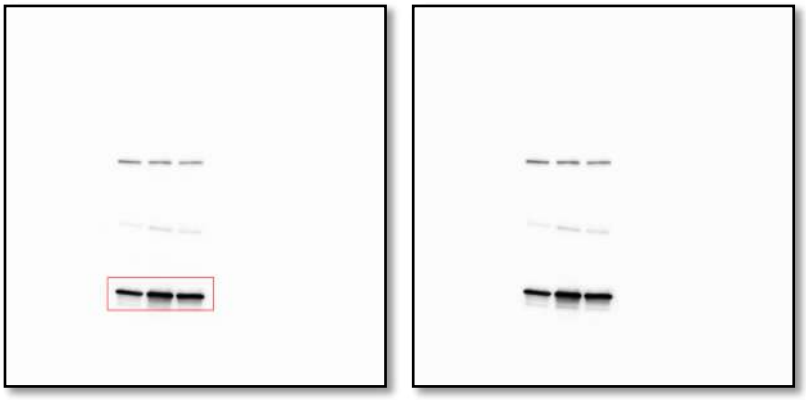

Western blot analysis of GAPDH protein levels in whole cell lysate of MCF7 cells expressing either the control vector or HTR2C.

Figure 5H_β-catenin in the nucleus_source data

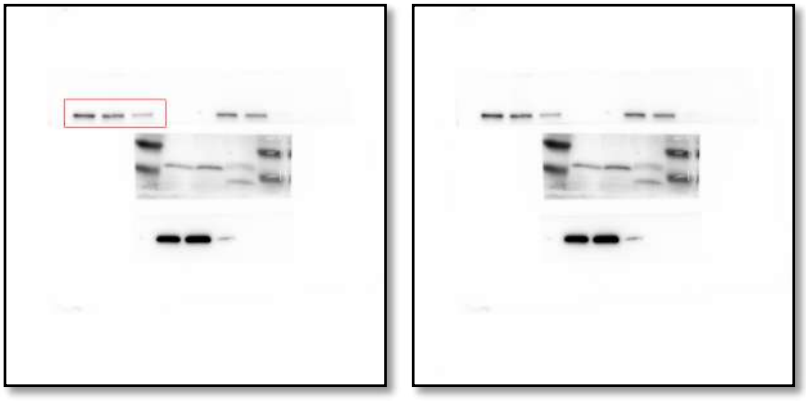

Western blot analysis of β-catenin protein levels in the nucleus of either vehicle or Pizotifen-treated MDA-MB-231 cells or E-cadherin positive cells in Pizotifen-treated MDA-MB-231 cells.

Figure 5H_Histone H3 in the nucleus _source data

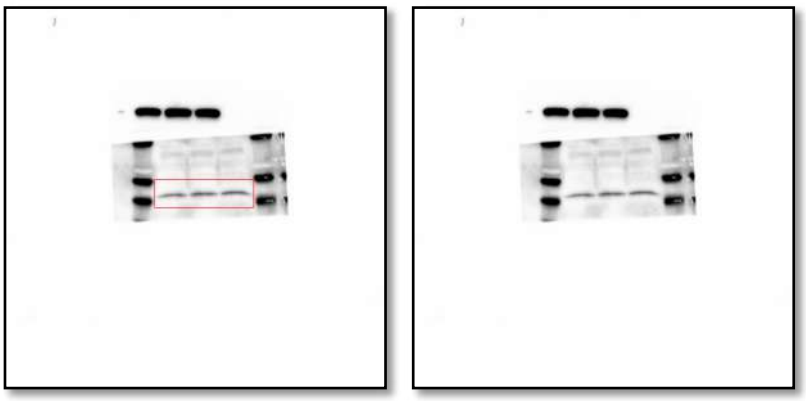

Western blot analysis of Histone H3 protein levels in the nucleus of either vehicle or Pizotifen-treated MDA-MB-231 cells or E-cadherin positive cells in Pizotifen-treated MDA-MB-231 cells.

Figure 5H_β-catenin in the cytoplasm_source data

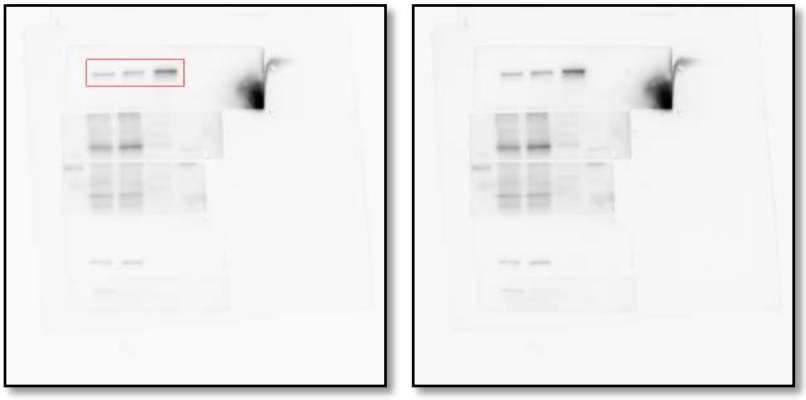

Western blot analysis of β-catenin protein levels in the cytoplasm of either vehicle or Pizotifen-treated MDA-MB-231 cells or E-cadherin positive cells in Pizotifen-treated MDA-MB-231 cells.

Figure 5H_β-tubulin in the cytoplasm_source data

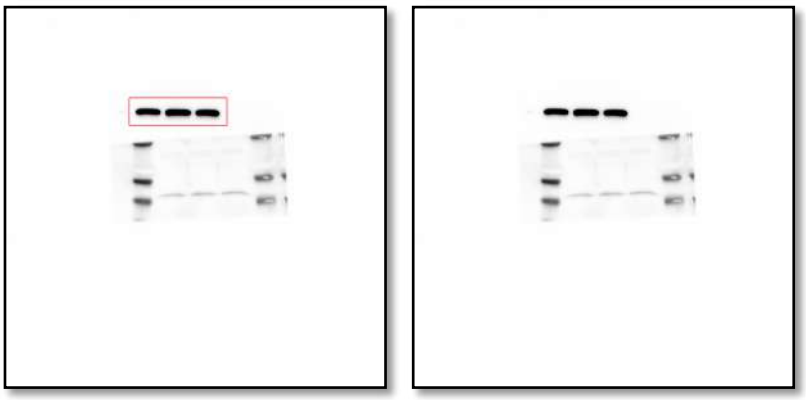

Western blot analysis of β-tubulin protein levels in the cytoplasm of either vehicle or Pizotifen-treated MDA-MB-231 cells or E-cadherin positive cells in Pizotifen-treated MDA-MB-231 cells.

Figure 5H_Phosphorylation of serine-9 in GSK3β_source data

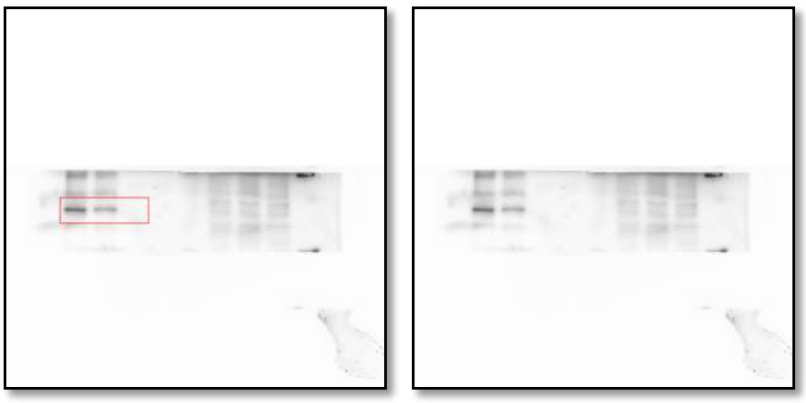

Western blot analysis of the protein levels of phosphorylation of serine-9 in GSK3β in whole cell lysate of either vehicle or Pizotifen-treated MDA-MB-231 cells or E-cadherin positive cells in Pizotifen-treated MDA-MB-231 cells.

Figure 5H_GSK3β_source data

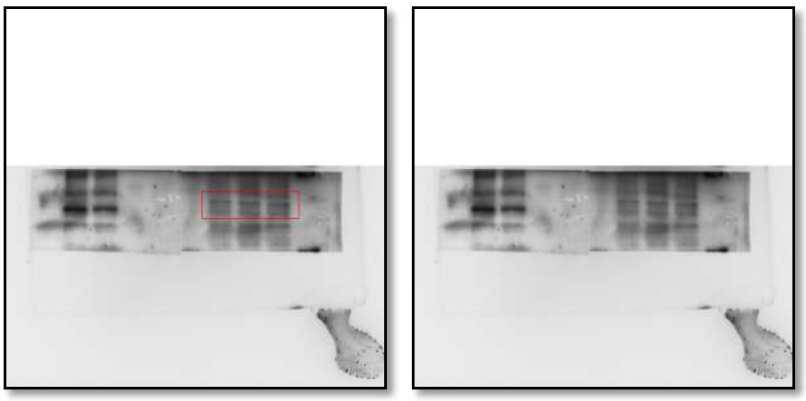

Western blot analysis of GSK3β protein levels in whole cell lysate of either vehicle or Pizotifen-treated MDA-MB-231 cells or E-cadherin positive cells in Pizotifen-treated MDA-MB-231 cells.

Figure 5H_GAPDH_source data

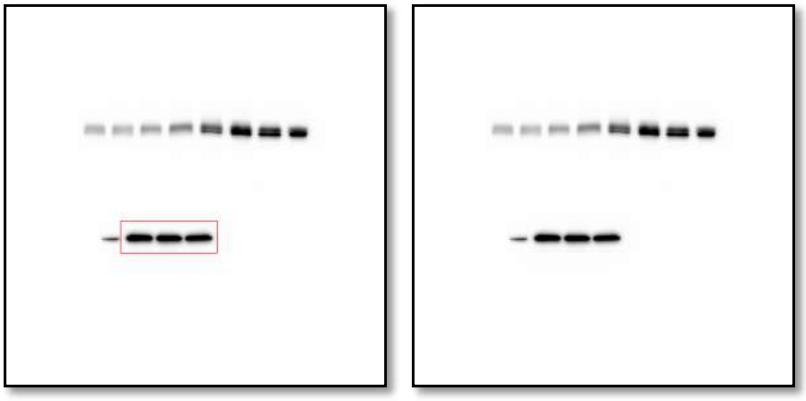

Western blot analysis of GAPDH protein levels in whole cell lysate of either vehicle or Pizotifen-treated MDA-MB-231 cells or E-cadherin positive cells in Pizotifen-treated MDA-MB-231 cells.

Figure S1A_ PRMT1_source data

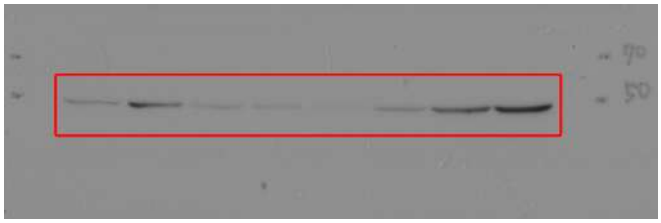

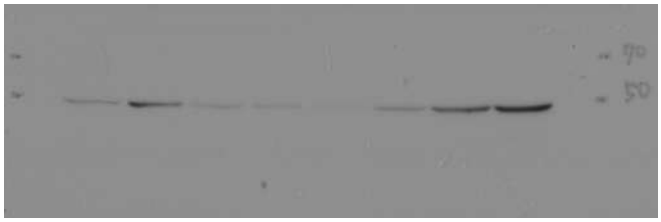

Western blot analysis of PRMT1 protein levels in non-metastatic human cancer cell line (MCF7) and highly metastatic human cancer cell lines (MDA-MB-231, MDA-MB-435, MIA-PaCa2, PC9, HCCLM3, SW620 and PC3).

Figure S1A_ CYP11A1_source data

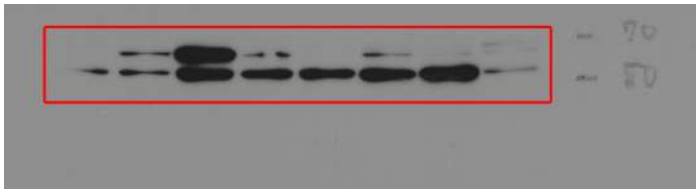

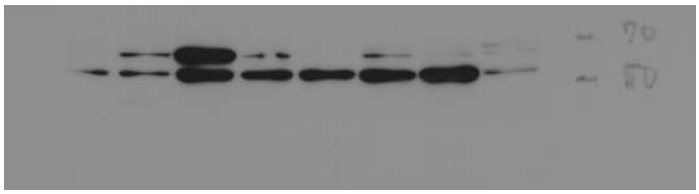

Western blot analysis of CYP11A1 protein levels in non-metastatic human cancer cell line (MCF7) and highly metastatic human cancer cell lines (MDA-MB-231, MDA-MB-435, MIA-PaCa2, PC9, HCCLM3, SW620 and PC3).

Figure S1A_ β-actin_source data

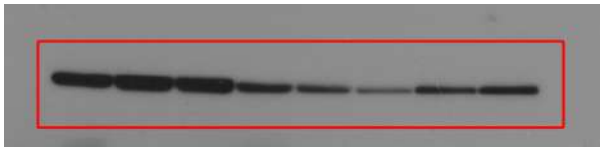

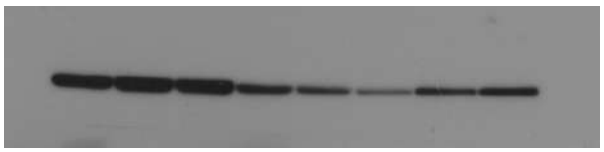

Western blot analysis of β-actin protein levels in non-metastatic human cancer cell line (MCF7) and highly metastatic human cancer cell lines (MDA-MB-231, MDA-MB-435, MIA-PaCa2, PC9, HCCLM3, SW620 and PC3).

Figure S1A_ PRMT1_source data

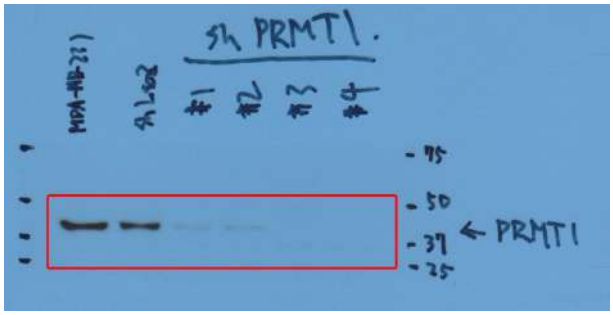

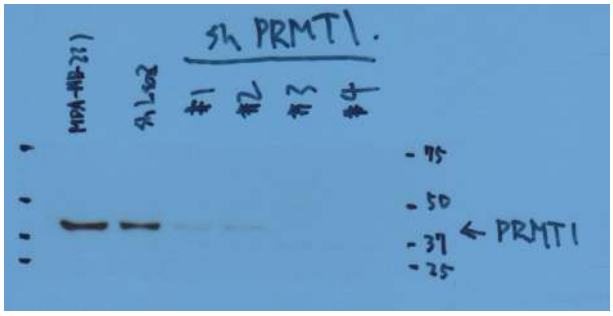

Western blot analysis of PRMT1 protein levels in sub-clones of MBA-MB-231 cells which were transfected with either a control shRNA targeting LacZ or one of four independent shRNAs targeting PRMT1 (clone #1 to #4).

Figure S1A_ β-actin _source data

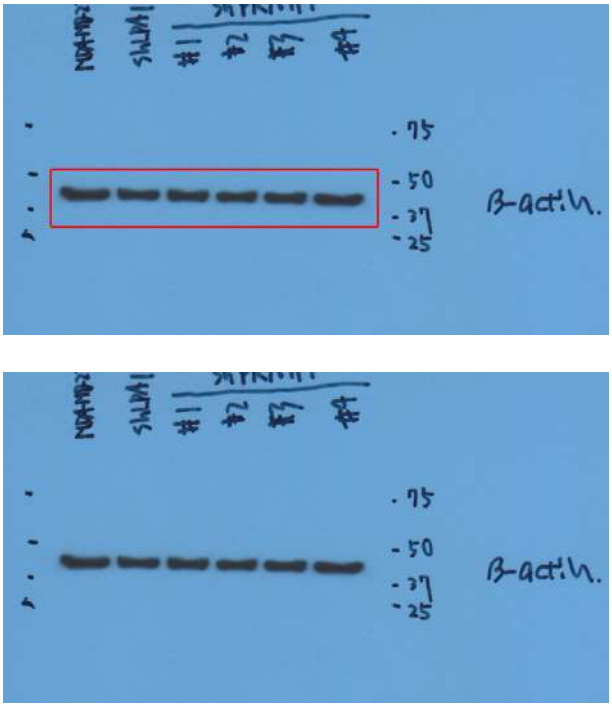

Western blot analysis of β-actin protein levels in sub-clones of MBA-MB-231 cells which were transfected with either a control shRNA targeting LacZ or one of four independent shRNAs targeting PRMT1 (clone #1 to #4).

Figure S1A_CYP11A1_source data

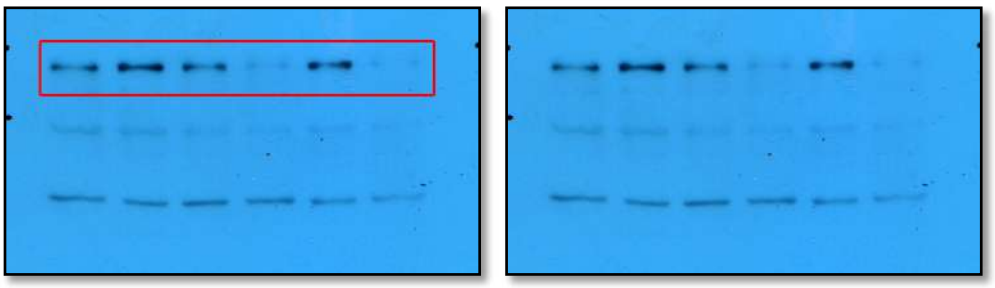

Western blot analysis of CYP11A1 protein levels in sub-clones of MBA-MB-231 cells which were transfected with either a control shRNA targeting LacZ or one of four independent shRNAs targeting CYP11A1 (clone #1 to #4).

Figure S1A_ β-actin_source data

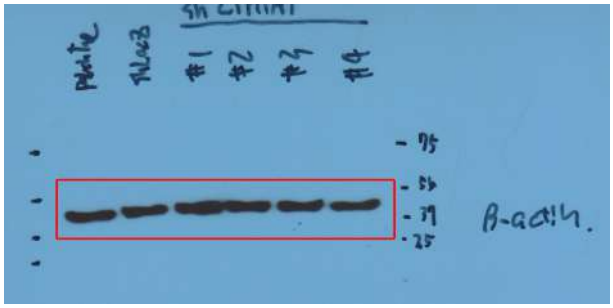

1332

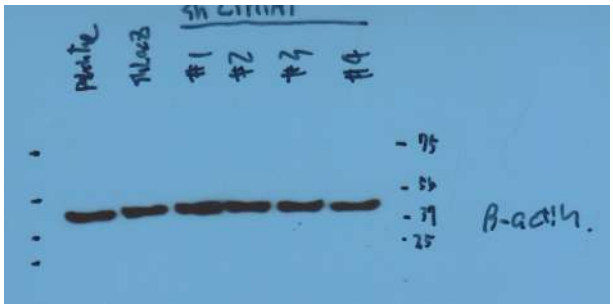

1333

1334 Western blot analysis of β-actin protein levels in sub-clones of MBA-MB-231 cells
1335 which were transfected with either a control shRNA targeting LacZ or one of four
1336 independent shRNAs targeting CYP11A1 (clone #1 to #4).

1337

1338 **Figure S2A_DRD2_source data**

1339

1340

1341 Western blot analysis of DRD2 protein levels in non-metastatic human cancer cell
1342 line, MCF7 (breast) and highly metastatic human cancer cell lines, MDA-MB-231
1343 (breast), MDA-MB-435 (melanoma), MIA-PaCa2 (pancreas), PC3 (prostate) and
1344 SW620 (colon)

1345

1346 **Figure S2A_GAPDH_source data**

1347

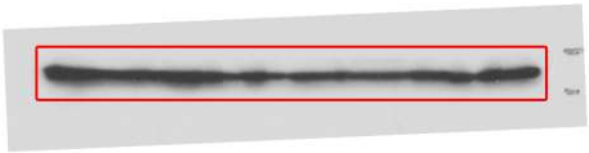

1348

1349 Western blot analysis of GAPDH protein levels in non-metastatic human cancer cell

1350 line, MCF7 (breast) and highly metastatic human cancer cell lines, MDA-MB-231

1351 (breast), MDA-MB-435 (melanoma), MIA-PaCa2 (pancreas), PC3 (prostate) and

1352 SW620 (colon)